

RESEARCH

Open Access



Antifungal activity of copper oxide nanoparticles derived from *Zizyphus spina* leaf extract against *Fusarium* root rot disease in tomato plants

Sozan E. El-Abeid^{1,2}, Mohamed A. Mosa^{1,2}, Mohamed A. M. El-Tabakh³, Ahmed M. Saleh⁴, Mohamed A. El-Khateeb^{5*} and Maha S. A. Haridy⁶

Abstract

Incorporating green chemistry concepts into nanotechnology is an important focus area in nanoscience. The demand for green metal oxide nanoparticle production has grown in recent years. The beneficial effects of using nanoparticles in agriculture have already been established. Here, we highlight some potential antifungal properties of *Zizyphus spina* leaf extract-derived copper oxide nanoparticles (CuO-Zs-NPs), produced with a spherical shape and defined a 13–30 nm particle size. Three different dosages of CuO-Zs-NPs were utilized and showed promising antifungal efficacy in vitro and in vivo against the selected fungal strain of *F. solani* causes tomato root rot disease, which was molecularly identified with accession number (OP824846). In vivo results indicated that, for all CuO-Zs-NPs concentrations, a significant reduction in *Fusarium* root rot disease occurred between 72.0 to 88.6% compared to 80.5% disease severity in the infected control. Although treatments with either the chemical fungicide (Kocide 2000) showed a better disease reduction and incidence with (18.33% and 6.67%) values, respectively, than CuO-Zs-NPs at conc. 50 mg/l, however CuO-Zs-NPs at 250 mg/l conc. showed the highest disease reduction ($9.17 \pm 2.89\%$) and lowest disease incidence ($4.17 \pm 3.80\%$). On the other hand, CuO-Zs-NPs at varied values elevated the beneficial effects of tomato seedling vigor at the initial stages and plant growth development compared to either treatment with the commercial fungicide or Trichoderma Biocide. Additionally, CuO-Zs-NPs treatments introduced beneficial results for tomato seedling development, with a significant increase in chlorophyll pigments and enzymatic activity for CuO-Zs-NPs treatments. Additionally, treatment with low concentrations of CuO-Zs-NPs led to a rise in the number of mature pollen grains compared to the immature ones. However the data showed that CuO-Zs-NPs have a unique antifungal mechanism against *F. solani*, they subsequently imply that CuO-Zs-NPs might be a useful environmentally friendly controlling agent for the *Fusarium* root rot disease that affects tomato plants.

Keywords Copper oxide, *Fusarium solani*, *Zizyphus spina*, Tomatoes, Enzymatic activity, Pollen grains

*Correspondence:

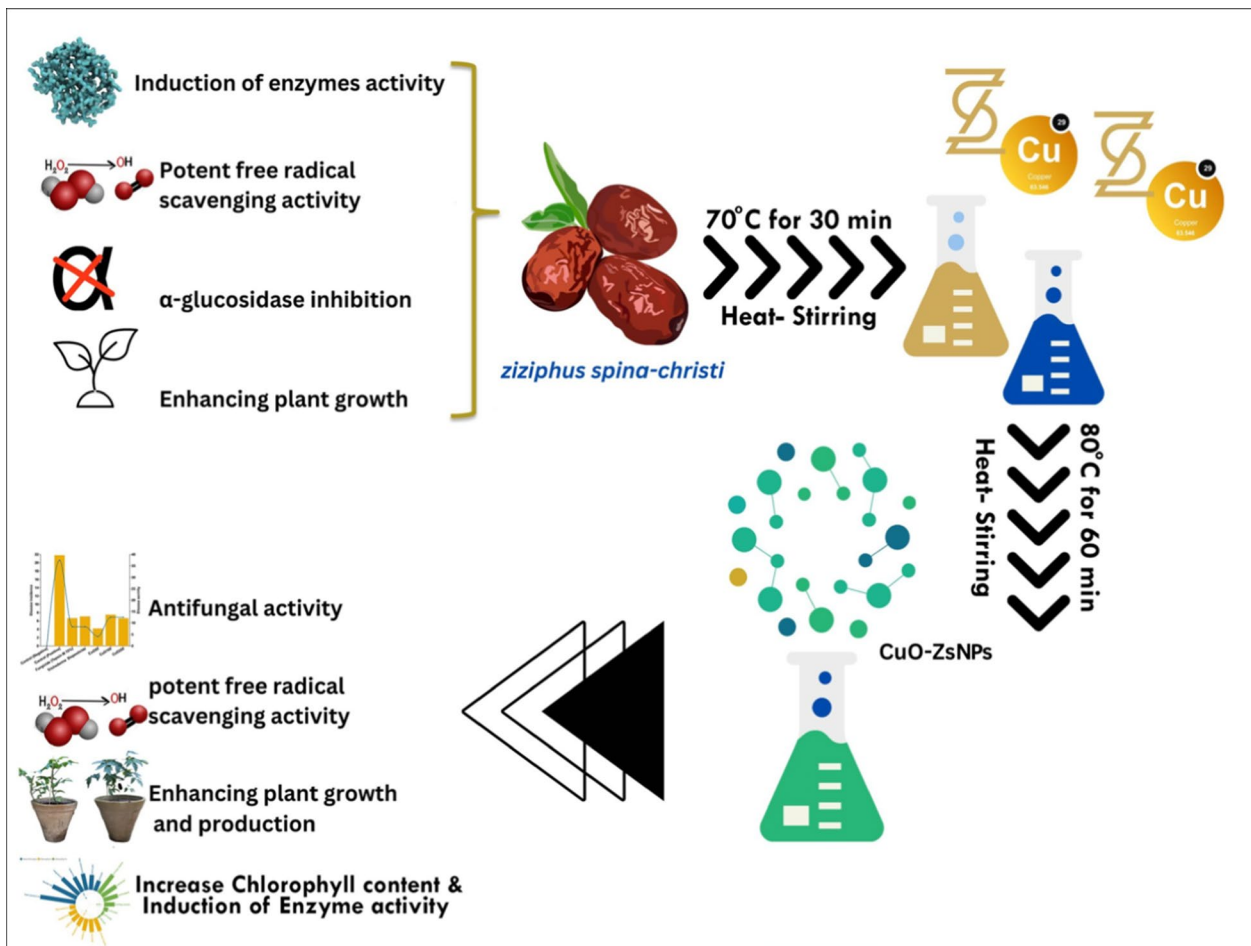
Mohamed A. El-Khateeb
elkhateebcairo@yahoo.com

Full list of author information is available at the end of the article



© The Author(s) 2024, corrected publication 2024. **Open Access** This article is licensed under a Creative Commons Attribution 4.0 International License, which permits use, sharing, adaptation, distribution and reproduction in any medium or format, as long as you give appropriate credit to the original author(s) and the source, provide a link to the Creative Commons licence, and indicate if changes were made. The images or other third party material in this article are included in the article's Creative Commons licence, unless indicated otherwise in a credit line to the material. If material is not included in the article's Creative Commons licence and your intended use is not permitted by statutory regulation or exceeds the permitted use, you will need to obtain permission directly from the copyright holder. To view a copy of this licence, visit <http://creativecommons.org/licenses/by/4.0/>. The Creative Commons Public Domain Dedication waiver (<http://creativecommons.org/publicdomain/zero/1.0/>) applies to the data made available in this article, unless otherwise stated in a credit line to the data.

Graphical Abstract



Introduction

Tomato plants (*Lycopersicon esculentum* L.) hold significant importance as a vegetable crop, contributing to a global production of 130 million tonnes [71]. In Egypt, tomato cultivation covers approximately 32% of the total cultivated land, with tomato crops accounting for an estimated 16% of all vegetables grown [20]. The United Nations Food and Agriculture Organization (FAO) reported that Egypt had a growing area of 173.28 ha that produced 6.752 million tons yield of tomato fruits [24]. However, many fungal infections may infect tomato plants from the ground up in the form of seeds. These infections severely impact crop output, leading to considerable economic loss [96], Hamza, Mohamed, and Derbalah [32]; [59, 76].

Fusarium is a notable fungal genus found in cropland soil, including various phytopathogenic species [58, 73]. Among these, the filamentous fungus *F. solani*, belonging

to the *Fusarium solani* (FSSC) species complex [16] and *Nectria haematococca* is the species' sexual form. They also cause root rot in crops such as tomatoes, leading to severe yield loss [16, 75]. Although crop rotation has been documented as a safe method for controlling soil-borne diseases such as *Fusarium solani* (Liu, Yang, and Du [52]), it is often ineffective due to varying climate conditions and economic benefits. The traditional approach of seed dressing and field application with classical chemical fungicides have been utilized to reduce and suppress some *Fusarium* diseases [60]; However, the adverse impacts of this chemical fungicide on the environment and human health have pushed farmers to focus on creating harmless agricultural management practices. Therefore, there is an urgent need to identify a viable and harmless strategy for preventing the spread and development of *Fusarium* root rot.

Copper biocides have been widely implemented in the management of crop diseases due to their broad antimicrobial spectrum and low cost. However, bulk Cu fungicides are easily agglomerated, resulting in a decrease in their antimicrobial activity [40]. Another pathway to environmental contamination is the production and use of traditional copper-based fungicides, especially in the ionic form. According to Keller and Lazareva [44], a significant proportion of copper, approximately 15%, produced through manufacturing processes is discharged into soil, potentially leading to contamination of agricultural land. This poses a critical concern for food safety, particularly for extensively cultivated and consumed crops, such as tomatoes. To address this problem, different reports have indicated that Cu-based compounds and their oxides at the nanoscale are more stable and less able to interact with ecosystem elements than their bulk materials reflecting greater enhanced antimicrobial activity [95]. In addition, copper nanoparticles (CuNPs) have been reported to promote growth and nutrient accumulation in certain plants treated with them [46, 66]. As a result, researchers are suggesting environmentally friendly methods of synthesizing materials, with biomolecules being favored over other agents due to their protective properties [26]. The biosynthesis of copper nanoparticles using plant extracts as reducing and capping agents due to reduced properties in the leaf or fruit extract has emerged as an important branch of nanoparticle synthesis when conventional physical and chemical methods are too expensive, risky, time-consuming, and labor-intensive. However, the phytotoxicity of various metal nanoparticles, including silver, zinc oxide, titanium oxide, copper, and ferric NPs, on tomato plants has been evaluated in different studies. Thus, further research is needed to compare their toxicity with that of their bulk equivalents (Karami [3, 14, 57, 64, 80]).

This study found that *Zizyphus spina-christi* (L.) wild leaves may effectively synthesize bioactive copper nanoparticles without negatively impacting the environment or the budget. Copper nanoparticles may be effectively reduced and stabilized using compounds in *Z. spina*-Christi leaves. This includes gallic acid, ellagic acid, hydrolyzable tannins, leucon anthocyanins, and flavanol glycosides (Cu-NPs). To our knowledge, no studies comparing the effects of nanocopper exposure to their bulk materials and Trichoderma-based biocides on soil-grown tomatoes have been undertaken. Therefore, the objectives of this study were to: (1) develop eco-friendly CuO NPs from *Zizyphus spina* leaf extract; (2) evaluate the antifungal properties of CuO-Zs-NPs against *Fusarium* root rot disease-causing agent under laboratory and greenhouse conditions; and

(3) Ascertain the copper-based nanoparticle translocation capability and short-term exposure consequences in complex soil media. To accomplish this, tomatoes were grown for 120 days in soil amended with three different concentrations of CuO-Zs-NPs; (3) evaluate the impact of CuO-Zs-NPs on (seed germination, plant height, (fresh, dry) plant weight, and fruit weights,); and (4) quantification of chlorophyll pigment content and the enzymatic activity (polyphenol oxidase, peroxidase, hydrogen peroxide (H₂O₂) scavenging) linked to the production of reactive oxygen species (ROS), which was chosen as the end objective for determining the effects of nano-copper exposure. Additionally, this study aims to fill the Knowledge gaps regarding the mechanisms underlying the impact of CuO-Zs-NPs on the tomato plant life cycle, specifically concerning their impact on yield and seed fertility.

Materials and methods

Analytical-grade chemicals were performed without any additional purification steps before use. Copper sulfate pentahydrate (CuSO₄·5H₂O, 98.0%), ammonia solution (NH₄OH), and Potato dextrose agar were all purchased from (PDA)Sigma-Aldrich Co. A pathogenic isolate of *Fusarium solani* (OP824846) was originally isolated from tomato plants infected with root rot, grown in sterilized culture tubes, and reserved for further study at 4 °C on a PDA medium.

Preparation of *Zizyphus spina Christi* plant extract:

Zizyphus spina Christi L (Zs) leaves were plucked from the Agricultural Research Center, garden, Egypt, and cleaned many times under running water to remove any remaining dust and dirt. Distilled water was used for flushing the leaves. In a 250 mL flask, 25 g of fresh leaves were combined with 100 mL of distilled water, and the resulting combination was heat-stirring at 70 °C for 30 min to produce an aqueous extract of the plant's leaves. After allowing the extract to cool to ambient temperature, it was filtered using Whatman No. 1 filter paper until it was completely clear. Freshly used within one week, the extract was refrigerated and employed to produce copper nanoparticles.

Synthesis of copperoxide nanoparticles

Approximately 10 mL of 25% aqueous extract from *Zizyphus spina Christi* was added gradually to 90 mL of 10 mM copper sulfate in a 250 ml Erlenmeyer flask to synthesize copper nanoparticles. For approximately 60 min, the mixture was heat-stirring continuously at 80 °C on a magnetic stirrer. CuO-ZsNPs were finally produced. This was preliminarily shown by the appearance of a dark green color, and the formed CuO-Zs-NPs solution was

centrifuged for 30 min at 6000 rpm, and the clear supernatant was discarded. To purify CuO-Zs-NPs, the generated pellets were washed three times with distilled water using repeated centrifugation, dried in a vacuum oven at 60 °C for 24 h, after that calcinated at 300 °C for 1 h and then subjected to characterization with some microscopic and spectroscopic analyses.

Characterization of copper oxide nanoparticles

The obtained CuO-Zs-NPs were confirmed through UV spectrophotometry (Thermo Spectronic, GENESYS-8, England, Quartz Cell, path length 10 mm). The hydrodynamic size distribution of the nanoparticles was determined using a Zeta Sizer Nano ZS Analyzer (Malvern Zeta Sizer Nano series, UK).

The morphology of the nanoparticles was observed by transmission electron microscopy (TEM, TECNAI 10Philips, Amsterdam, Netherlands).

Furthermore, to study the functional groups of CuO-ZS-NPs, the FT-IR spectrum was determined in the transmission mode (4000–400 cm^{-1}) using a BOMEM FT-IR spectrometer (MB 147, Canada on KBr disk), a data library provider. A powder sample of approximately 100 mg was put in spectral grade KBr and pressed into discs under hydraulic pressure.

Isolation and molecular identification of *Fusarium* isolate

During the summer of 2021, tomato plants exhibiting symptoms of *Fusarium* root rot were collected. Stem sections (3–5 cm in length) displaying root rot symptoms were thoroughly washed with tap water and then surface-disinfected for two minutes with a 2% chlorine solution. The small pieces were thoroughly rinsed with sterile double-distilled water (ddH_2O) and then left to dry on filter paper under sterilized conditions before being placed into PDA medium (Potato + Dextrose + Agar) amended with 300 $\mu\text{g}/\text{ml}$ streptomycin sulfate. Fourteen days were spent in a 25 ± 2 °C incubator with the fungal cultures. DNA analysis corroborated the fungal's phylogenetic position after they were identified following specified mycokeys after a light microscope examination [35, 63]. The isolated *Fusarium* species was first cultivated on a PDA medium at 27 °C for 14 days to achieve molecular identification. The produced fungal mycelia were prepared as previously described [18]. The fungal DNA extraction was performed as stated by the steps of the DNeasy plant mini kit recommendation (Qiagen, Hilden, Germany).

Molecular identification of *Fusarium solani*

The *F. solani* isolate was molecularly identified using the same PCR mixture and temperature conditions outlined to ensure its accuracy [18]. In addition, the ITS1

and ITS4 primers were used to amplify and sequence the ITS region of rDNA [98]. Two microliters of genomic DNA (10 ng/L), half a microliter of each primer pair (0.5 mM), and twelve and a half microliters of master mix (OmniPCR (MBA01-0100)) were used in a total volume of twenty-five microliters [15]. Initially, the amplification program consisted of a denaturation cycle for 3 min. at 94 °C followed by 35 cycles (at 95 °C for 15 s, 53 °C for 30s. and 72 °C for 80 s). Finally, the extension step was 72 for 10 min. The obtained PCR product was visualized by electrophoresis on a 2% agarose gel. Using identical forward and reverse primers, the purified PCR products were sequenced. The experimental sequences for *F. solani* isolate have been deposited in the GenBank repository (NCBI).

The activity of CuO-Zs-NPs against *Fusarium solani* in vitro

The produced Cu-Zs-NPs were tested for their antifungal activity against *F. solani* using the agar dilution method described in [59]. In this regard, 1mL of each concentration (50, 100, 250 mg/l) of CuO-Zs-NPs was supplemented separately in sterilized Petri plates containing 8 ml of sterilized melted PDA medium. The two solutions were mixed in a gentle circular motion to become homogenized before solidification. The commercial chemical fungicide “Kocide 2000, 2.5 $\mu\text{g}/\text{mL}$ conc.” and Trichoderma Biocide *Trichoderma viride* 1.5% W.P. (One colony from a 7 days-old culture was inoculated in a 500 ml Erlenmeyer flask with 100 ml PDB to make biocide CFU count of $2 \times 10^6/\text{gm}$ minimum) served as controls to compare its activity with the produced CuO-Zs-NPs, while untreated plates were used as negative controls in this study. The flask was shaken at 200 rpm in an incubator at 27 °C for 7–10 days. To obtain cell-free supernatant, the *Trichoderma* culture was centrifuged for 15 min at 10000 rpm and filtered. Inoculating a Petri plate with 1 ml of cell-free supernatant, and then adding 8 ml of media). Thereafter, to evaluate the antifungal effect of CuO-ZS-NPs treatments on *F. solani*, a small disc (0.5 cm diameter) of active mycelial growth from the edge of an 8-day-old fungal culture was placed in the center of each prepared plate. The plates were then incubated at 26 ± 2 °C for 10 days. The radial growth of fungal hyphae was measured in all inoculated plates to determine the inhibition percentage using the formula:

$$\text{Inhibition (\%)} = T - t/T \times 100.$$

where(T) is the radial growth of fungal hyphae on the control plate and (t) is the radial growth of fungal hyphae in treatments [18]. All in vitro experiments were conducted in triplicate under sterile conditions to ensure the accuracy and reliability of the results.

CuO-Zs-NPs phytotoxicity test

Germination assays

Tomato seeds were subjected to surface disinfection using a 2.5% NaOCl solution, followed by triple rinsing with distilled, sterilized water and air drying. To evaluate germination, 9 ml plates containing sterilized filter paper amended with various concentrations of CuO-Zs-NPs (50, 100, and 250 $\mu\text{g}/\text{mL}$), Kocide 2000 (a commercial fungicide) (Certis, Columbia, MD, USA), and Trichoderma Biocide were used under aseptic conditions at the recommended dose. Twenty-five seeds were placed on the surface of the sterilized filter paper in each plate (4 replicates/treatment) using sterilized forceps to ensure contact with the medium. The plates were incubated for six days at $25\text{ }^{\circ}\text{C} \pm 2$ in a growth chamber with a 16 h:8 h day: night photoperiod. The experiment was repeated twice using twenty plates per treatment. The germination percentage (GP %) was calculated as follows: GP (%) = treatment average of germination seed / control average of germination seed $\times 100$.

Greenhouse experiments

Preparation of soil medium

To investigate the impact of nano-copper exposure on tomato plants under sterile conditions, a soil medium consisting of loamy sand soil mixed with deionized water was prepared. The soil was amended with varying concentrations of CuO-Zs-NPs (50, 100, and 250 $\mu\text{g}/\text{mL}$), the chemical fungicide Kocide 2000 (Certis, Columbia, MD, USA), and Trichoderma Biocide. The pH of the soil was 7.9 [97]. The mixture was thoroughly mixed until homogeneity was achieved and allowed to settle for 24 h. Subsequently, four pots per treatment were filled with 0.5 L of the soil mixture, and three tomato seeds were planted in each pot. All pots were then transferred to environmentally controlled growth chambers for three weeks under a temperature cycle of 25/20 $^{\circ}\text{C}$ day/night, relative humidity of 65–70%, and a photoperiod of 14 h with a light intensity of $340\text{ }\mu\text{mol m}^{-2}\text{ s}^{-1}$.

Effect of CuO-Zs-NPs on seed germination and plant growth

The efficacy of CuO-Zs-NPs on seed germination and some plant growth parameters of *Lycopersicon esculentum* L. plants was evaluated under greenhouse conditions. In this regard, ten seeds/replicates of tomato plants were first sterilized for 1–2 min in a solution of sodium hypochlorite (0.25% w/v). Seeds were then rinsed multiple times with ddH₂O. Then, they were grown in small sterilized plastic bags filled with sterilized peat moss (0.5 kg) and treated individually with three different concentrations (50, 100, 250 $\mu\text{g mL}^{-1}$) of CuO-Zs-NPs under greenhouse conditions. Additionally, treatment with both

the chemical fungicide Kocide 2000 and Trichoderma Biocide was also used to compare their efficacy on seed germination and plant growth in comparison to CuO-Zs-NPs treatments and the nontreated tomato seed “control”. All treatments were evaluated in triplicate (3 pots in each replicate and 10 seeds/pot) at the 3–5 leaf stage, to study their efficacy on seed germination, seedling height, and seedling vigor index according to the following equation [50].

Vigor index (VI)

$$= [\text{seedling length (cm)} \times \text{seed germination rate}]$$

Fungal inoculum preparation

To assess the effectiveness of CuO-Zs-NPs against *Fusarium* root rot, an inoculum suspension of *F. solani* was prepared using potato dextrose broth according to the method of Tesso et al., [83] with some modifications. The spore suspension was shaken and incubated at 160 rpm, and 30 $^{\circ}\text{C}$ for six days. After that the spore suspension was filtered and a sterile phosphate-buffered saline (PBS) solution was used to bring the spore concentration to the target value (1×10^6 conidia mL^{-1}).

In vivo experiments

Antifungal analysis of CuO-Zs-NPs against *Fusarium* root rot

The effectiveness of CuO-Zs-NPs in combating *Fusarium* root rot caused by *F. solani* was assessed in a greenhouse experiment using a susceptible strain of tomato (cv. TH99806). Three replicates of each treatment were conducted, with four to five seedlings in each replicate, using 25 cm diameter plastic pots filled with three kilograms of sandy, loamy soil mixed at a ratio of 1:1 (v:v) and autoclaved twice for thirty minutes at 121 $^{\circ}\text{C}$. Each container was infected with 30 mL of a fungal spore solution containing 1×10^6 conidia mL^{-1} a week before the seedlings were transplanted. Tomato seedlings were subsequently exposed to varying concentrations of CuO-Zs-NPs (50, 100, and 250 g mL^{-1}). Distilled water was used as the negative control, while Trichoderma Biocide and Kocide fungicide (2.5 g/L) were used as the positive controls. Then the treatments were repeated 30 days later. Every four weeks, 1 g L^{-1} of soluble NPK fertilizer was applied to the plants, and the plants were constantly examined for disease symptoms. After 45 days, growth data including plant length, biomass weight (Fresh + dry), as well as disease incidence (DI), and severity (DS) were recorded. Fresh biomass (g) was determined by removing excess soil from seedlings and their roots, whereas dry biomass (g) was determined by drying them in a vacuum oven at 60 $^{\circ}\text{C}$ for three days. The severity of root rot disease was evaluated according to Romberg and Davis

[72], using the following scale (0–4) with minor modifications. Disease severity rating scale (Showing brown taproots with slight to severe internal browning at the root tip): 0 = asymptomatic-healthy plants (none), 1 = less than 20%, 2 = 20–50%, 3 = > 50–75% browning taproots (severe), and 4 = > 75–100% leaves and roots with infection, total plant death, and drying.

The severity of the disease was determined using the following formula:

$$\text{Severity (percentage)} = \frac{P \times (n \times V)}{4 \times N} \times 100$$

N is the total number of plants tested for each treatment, **P** is the number of infected plants, **V** is the score of disease index, and 4 is the highest rate of disease index. Additionally, the following formula was used to determine disease incidence (DI):

$$\text{DI} = \left(\frac{\text{Number of dead plants}}{\text{Total number of plants}} \right) \times 100$$

Tomatoes were picked when mature on the 80–105th day following transplanting, at which point their uniformity and lack of damage could be verified, and the average fruit weight per plant was determined. On the 80–105th day after transplantation, tomatoes were harvested at the ripening stage, confirming that they were uniform and undamaged, and the average fruit weight per plant was also calculated.

Physiological studies

Estimation of plant height, fresh and dry weight, fruit weight and Chlorophyll contents

In all treatments, the growth parameters and physiological effects of CuO-Zs-NPs on tomato plant height, fresh dry weight, fruit weight, and the level of certain photosynthetic pigments (chlorophyll a, b, and total chlorophyll content) were also assessed. For chlorophyll estimation, approximately 100 mg of leaf tissues from each set of treatments, including the mock-treated control, were weighed and extracted with 80% acetone in water (v/v) until the chlorophylls were completely released into the solution. Afterward, the suspensions were filtered, and absorbance at wavelengths 644 and 663 nm was measured. The concentration of photosynthetic pigments was evaluated based on Venkatachalam et al. [88]. Using the equations published by Lichtenthaler [51], chlorophyll a, b, and total chlorophyll were determined and expressed as mg/g-1 FW. Chlorophyll a = $12.25 \times A_{663} - 2.79 \times A_{645}$ chlorophyll b = $21.50 \times A_{645} - 5.10 \times A_{663}$.

Estimation of enzymatic activities

Estimation of polyphenol oxidase (PPO)

To measure PPO activity, we used a technique originally developed by Kar and Mishra [39] with some modifications. We centrifuged 1 g of leaf tissue at 10,000×g for 25 min at 4 °C after homogenizing it in 2 mL of 0.1 M sodium phosphate buffer (pH 6.5). The enzyme extract was prepared from the supernatant. The 3 mL of reaction mixture included 0.1 mM pyrogallol, 25 mM phosphate buffer (pH 6.8), and 0.1 mL enzyme extract. The reaction mixture was left without pyrogallol for calibration. The absorbance at 420 nm was recorded for each specimen.

The peroxidase (POD) activity

The approach presented by Gong et al. [29] was used to estimate the provided sample. Initial steps included grinding 1 g of leaf tissue in 5 ml of 0.05 M phosphate buffer (pH 7.0) containing 10% polyvinylpyrrolidone (PVP-SIGMA) and 0.1 M ethylene di-amine-tetra-acetic acid (EDTA-SIGMA). To utilize the supernatant for the POD test, the resultant mixture was centrifuged at 14,000 rpm for 20 min at 4 °C. The approach of Vetter et al. [89] was used to measure POD activity, with some adjustments made by Gorin and Heidema [30]. A 0.1 mM 2-morpholino ethane-sulfonic acid (MES) buffer, 0.05% hydrogen peroxide (H₂O₂), 0.10% phenylenediamine, and 0.10 ml (mL) of enzyme extract were used in the test combination (pH 5.5). Each sample's absorbance changes at 485 nm were recorded for 3 min.

Hydrogen peroxide (H₂O₂) scavenging percentage

The percentage of hydrogen peroxide scavenging was determined from a methanolic leaf extract solution at a concentration of 1mg/10 ml and measured at 230nm wavelength according to the protocol of Eswaran, et al. [21]. In this regard, 1ml of the extract solution was gently mixed with 0.6ml (40mM) H₂O₂ prepared in phosphate buffer (pH 7.4). The final complete volume was 3 ml followed by incubation for 10 min at room temperature. Blank samples consisting of phosphate buffer without H₂O₂ were used in this experiment. The percentage of H₂O₂ scavenging in plant samples was calculated as indicated by Eswaran, et al. [21], following the equation:

$$\text{H}_2\text{O}_2\text{scavenging (\%)} = \frac{(A_0 - A_1) \times 100}{A_0}$$

where, **A₀** is the absorbance of the control samples, and **A₁** is the absorbance of the treated samples.

Determination of Cu Content in Tomato terminal apical tissues

The concentration of the elemental Cu was determined, as described by Hernández-Hernández et al. [34]. First, tomato terminal apical tissues were harvested at maturation (120 days) and rinsed properly to remove the soil and dust particles, followed by extensive washing with distilled water and Air drying. The dried tissues were oven-dried at 50 °C for 72 h and gently ground to a fine powder. The digestion of 0.2 g of dry materials for analysis of Cu content was carried out by adding 30 ml of concentrated HNO₃ to a 100 ml beaker. The beaker was covered with a watch glass and heated on the grill for approximately four hours until complete disintegration of the organic substance was achieved. The volume of HNO₃ was adjusted periodically to prevent sample drying. Upon achieving a clear solution with no residue, the solution was cooled and filtered using Whatman No. 42 filter paper. The resulting filtrate was diluted with deionized water to a final volume of 50 ml in a volumetric flask. Subsequently, 1: 10 dilutions were prepared and analyzed for total Cu content using an inductively coupled plasma atomic emission spectrometer (ICP, ThermoJarrell Ash model 7400).

Effect of Cu treatments on pollen grains

For the purpose of analyzing pollen grains, a number of flower bud samples were harvested from all treated and non-treated tomato plants. In this regard, flower buds of reliable size were randomly selected and fixed in a freshly made Carnoy's fixative solution (mixture of ethyl alcohol, chloroform, and glacial acetic acid in a volume ratio of 6:3:1). The anthers were then stained with 1% aceto carmine staining solution. The fertility of pollen was evaluated using stain-ability tests.

Staining of pollen grains was used as a proxy for fertility; unstained or crushed pollen was considered sterile; and bursting pollen grains were also included in the count [19, 33].

The size of pollen grains that measured 1.5 times larger than the normally reduced pollen (n) in diameter was considered as unreduced (2n) pollen. Freshly visible pollen grains with clear characteristics were finally photographed using a HiROCAM (High-Resolution Optics Camera) digital imaging microscope eyepiece system [47].

Statistical analysis

One-way analysis of variance (ANOVA) was performed on the collected data [7]. Using SPSS software version

22.0, means were compared using the Least Significant Difference (LSD) test ($P < 0.05$). The data shown here is the average of the three sets of results from each experiment, repeated three times (SD). The ability to visualize data are made available when utilizing MINITAB V.14 with R-studio V.4.1.3. GraphPad Prism 9 software was also used to make and edit graphs. The particle size was measured using Image J (version 1.53f), and Origin 2018 was used to create the particle size distribution histogram.

Results and discussion

Green synthesis of CuO-Zs-NPs

For the CuO-Zs-NPs to be formed, a solution of 90 mL copper sulfate was mixed with 10 mL of *Zizyphus spina* leaf extract at a ratio of 9:1 (v/v) and stirred continuously for 60 min at 80 °C. The color of the solution changed from blue to dark green during the reaction, indicating the formation of CuONPs. This was confirmed using UV-vis spectroscopy, which showed the electronic spectrum caused by the surface plasmon resonance (SPR) effect [2, 5, 12, 28]. Previous studies have also reported the functional role of tannins, saponins, phenols, and alkaloids present in *Zizyphus spina* aqueous extract which was used as capping and stabilizing agents for green synthesis of CuO-Zs-NPs and their possible involvement in reducing Cu⁺ to Cu⁰ [1, 45, 68, 93]. The mechanism for the synthesis is illustrated in Fig. 1.

Characterization of the biosynthesized copper oxide nanoparticles (CuO-Zs-NPs)

UV Absorption of CuO-NPs

By analyzing the UV-visible spectrum, a strong absorption peak located at approximately 290 nm was observed, which represents the successful synthesis of CuO nanoparticles (NPs) (Fig. 2A). The peak position and width are related to the average size and size distribution of the nanoparticles, respectively. This peak is attributed to the inter-band transition of core electrons in copper and the band gap difference associated with quantum size effects, which is consistent with the formation of various CuO NPs [27]. Furthermore, the absorption peak of excited CuO NPs that was noticed at 290 nm at a temperature of 23 °C, indicates a mono-dispersed size distribution in the mixture [69]. These results are compatible with those reported by Jing et al. (2019), which demonstrate the formation of stable CuO NPs [62].

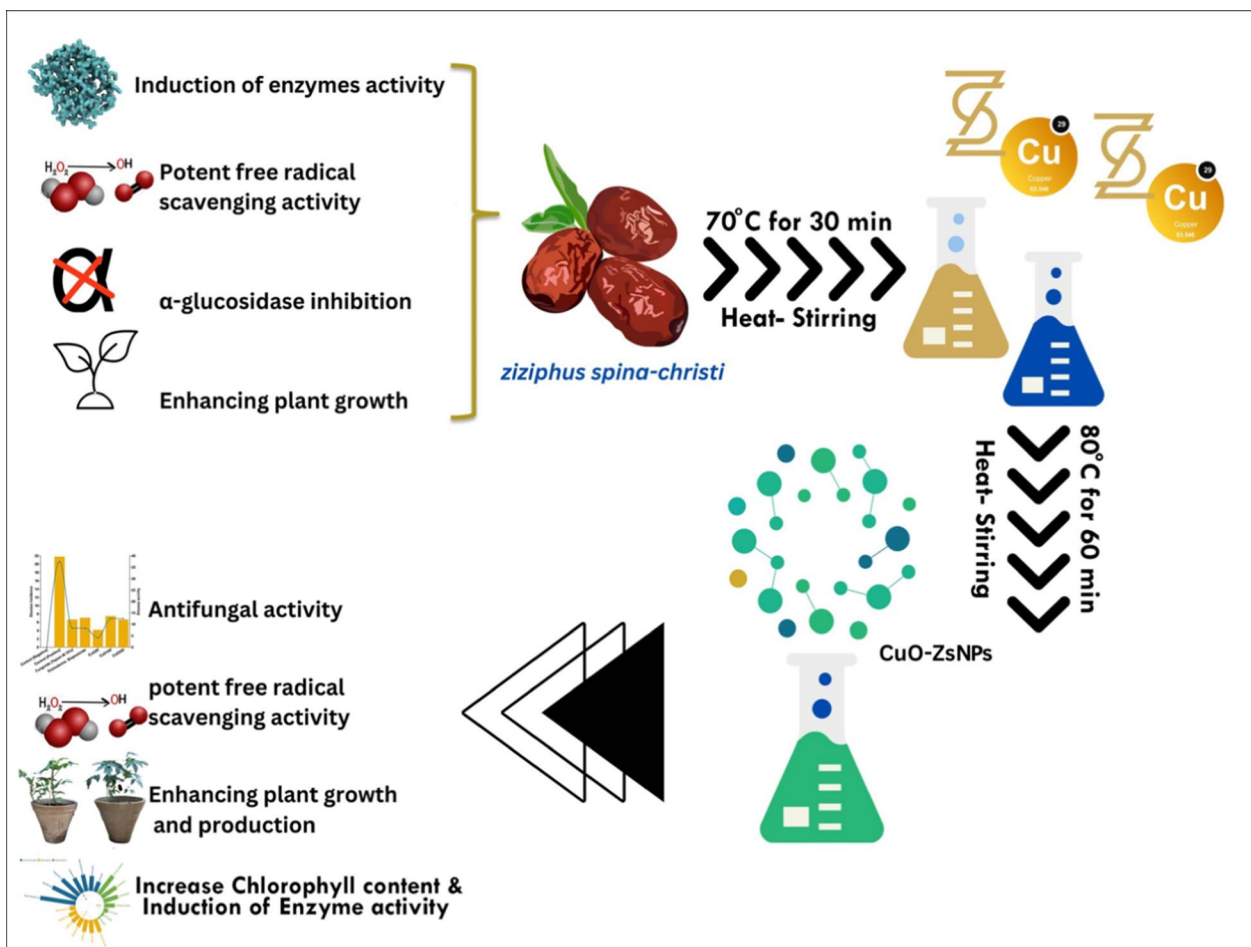


Fig. 1 A schematic representation showing the possible mechanism for synthesizing the CuO-Zs- NPs

Morphology and size distribution of CuO-NPs

The morphology and size distribution of CuO-Zs-NPs nanoparticles (NPs) synthesized via a biosynthetic pathway were examined using Transmission Electron Microscopy (TEM), a crucial characterization technique for obtaining quantitative measures of particle size, size distribution, shape, and lattice fringes. The TEM image showed the appearance of spherical-shaped CuO-Zs-NPs with a particle size range of 13.4 – 30.9 nm (Fig. 2C). The size distribution measurements by dynamic light scattering were found to agree with the TEM analysis, yielding a particle size of mean at 34.1 ± 4.379 nm (Fig. 2B).

However, slight variations in the two measurements can be due to many of variables. Dynamic light scattering (distribution analysis) investigates the hydrodynamic particle diameter in solution, which is based on the Brownian motion of particles in a solvent. Furthermore, temperature, viscosity, and particle translational diffusion coefficient all influence the hydrodynamic diameter in the solvent. The hydrodynamic diameter also takes account of all of the molecular sizes and hydration layers of water molecules.

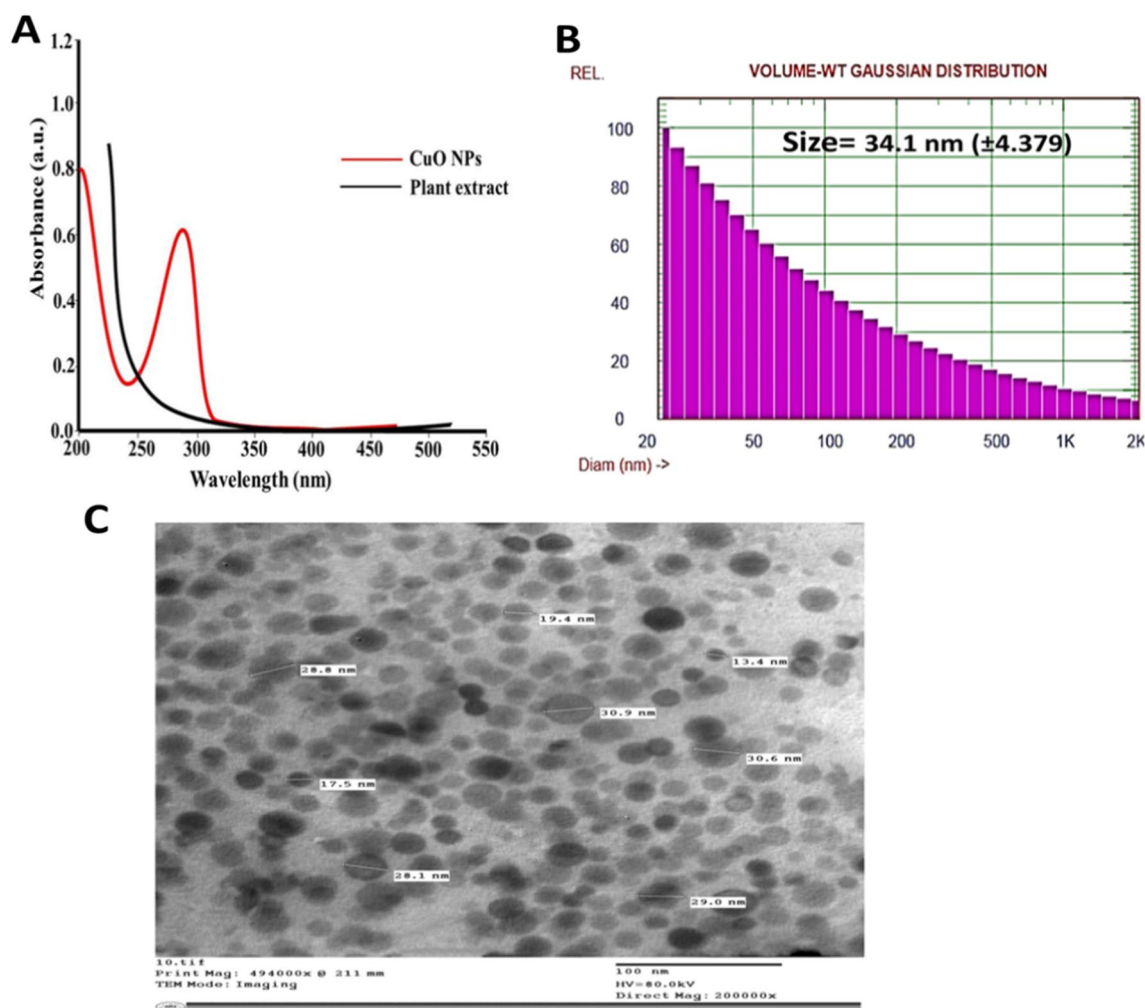


Fig. 2 Characterization of the produced CuO-Zs-NPs: **A:** UV-vis spectroscopic analysis of the produced CuO-Zs-NPs and plant extract, **B:** Distribution analysis of CuO-Zs-NPs size, and **C:** Transmission electron microscope (TEM) image of the formed CuO-Zs-NPs

FT-IR analysis

To further examine the phytochemicals of *Zizyphus spina* leaf extract and their potential chemical functional groups responsible for the reduction and stabilizing of the CuO-Zs-NPs, FT-IR analysis was also performed on the produced CuO NPs to determine their chemical structure. As depicted in Fig. 3, the FT-IR spectrum shows absorption bands of *Zizyphus spina* leaf extract centered at 3448.99, 2063.66, 1635.32, 1559.35, 1417.91, 1035.30, 867.98, 701.67, 676.9, 647.76 and 470.7 cm^{-1} (Fig. 3A). The broad absorption band at 3448.99 cm^{-1} may be attributed to the stretching vibrations of (–OH), while the peak at 2063.66 attributed to alene (C=C), and 1635.32 cm^{-1} may be attributed to the amine orenone group. While The peak at 1559.35 is due to the C=C stretching of the aromatic ring, in tertiary amides, flavonoids, terpenoids, tannins, and saponins. In addition, the peak at 1417 cm^{-1} could be due

to C-N stretching in imines or oximes, or C-N stretching in aliphatic amines and 1035.30 are associated with C-O stretching in alcohols, phenols, ethers or esters also be due to C-N stretching in aromatic amines.

In Fig. 3B, the FT-IR absorption bands of CuO-Zs-NPs were centered at 3188.67, 2345.33, 2153, 2093, 1959, 1613, 1414, 1063, 605, and 453 cm^{-1} (Fig. 3B). The broad absorption band at 3188.67 cm^{-1} may be attributed to the stretching vibrations of (–OH), while the peak at 2345.33 attributed to Carbon dioxide (O=C=O), and 2153 cm^{-1} may be attributed to the presence of Si-based compounds. The peak at 1613 is due to N–H bending in primary amides, such as amino acids, and the C=C stretching in tertiary amides— flavonoids, terpenoids, tannins, and saponins. In addition, the peak at 1414 cm^{-1} could be due to C=N stretching in imines or oximes, or C-N stretching in aliphatic amines, and 1063 could be associated with

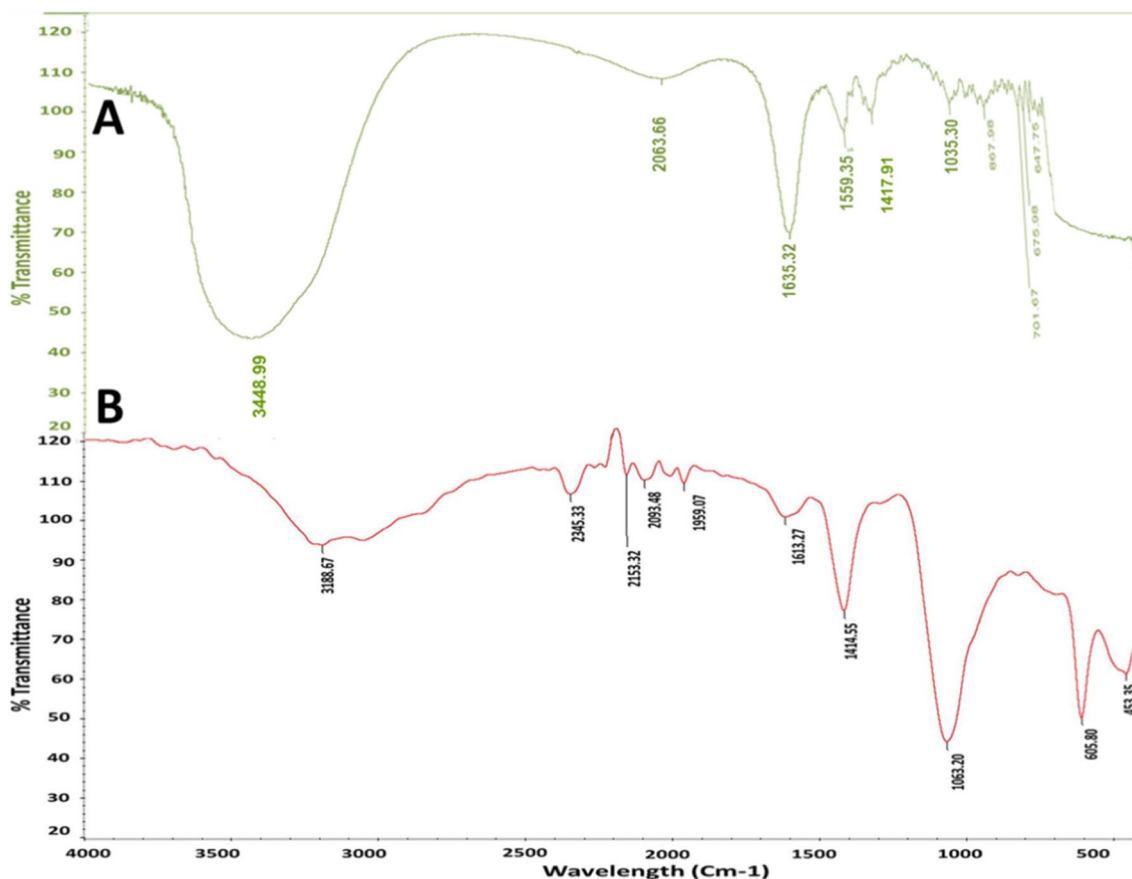


Fig. 3 FT-IR spectrum analysis of *Zizyphus spina* leaf extract (A) and the formed CuO-Zs-NPs (B)

C-O stretching in alcohols, phenols, ethers or esters also be due to C-N stretching in aromatic amines. Whereas the peak at 605 and 453 indicate the formation of O bonds, these data were attributed to [37].

Molecular identification of *Fusarium solani*

Molecular identification of the causal agent of tomato root rot disease was performed using the internal transcribed spacer (ITS) region of ribosomal DNA. The ITS sequence of the isolated fungal strain showed 100% similarity with *F. solani* isolate sequence with the accession number (MW216959.1) available on the GenBank database. The identified ITS region of *F. solani* isolate was then assigned in the GenBank database with the accession number (OP824846).

In vitro antifungal activity effect of CuO-Zs-NPs

CuO-Zs-NPs anti-fungal activity was tested at various concentrations (50, 100, and 250 $\mu\text{g}/\text{mL}$), which are referred to in the manuscript as (CuO50,

CuO100, and CuO250) respectively, in comparison with their bulk precursor of copper "Kocide 2000" as the chemical fungicide and TricodermaBiocide in terms of mycelial growth inhibition against isolated *F. solani* in vitro. The antifungal activity of CuO-Zs-NPs increased with increasing concentration (Fig. 4). Specifically, the highest levels of growth inhibition were achieved at a concentration of 250 mg/l for CuO-Zs-NPs. With a significant value of 91.17 ± 1.28 , compared to Kocide 2000 as a chemical fungicide and the Trichoderma Biocide (*Trichoderma viride* 1.5% WP) showed values 88.20 ± 3.57 and $77.09 \pm 5.88\%$ after ten days of incubation (Table 1; Fig. 4). Interestingly, statistical analysis indicated that when examining the antifungal effect of the three tested CuO-Zs-NPs concentrations, the NPs concentration is a significant factor. Furthermore, this is in agreement with several studies showing that CuO-NPs display multiple inhibitory modes of action against microbial pathogens [31]. Additionally, Lopez-Lima et al. [53] tested Cu-NPs at different doses for *in-vitro* antifungal activity against *Fusarium oxysporum* f. sp. *lycopersici* (FOL). In addition, 0.5 mg/mL

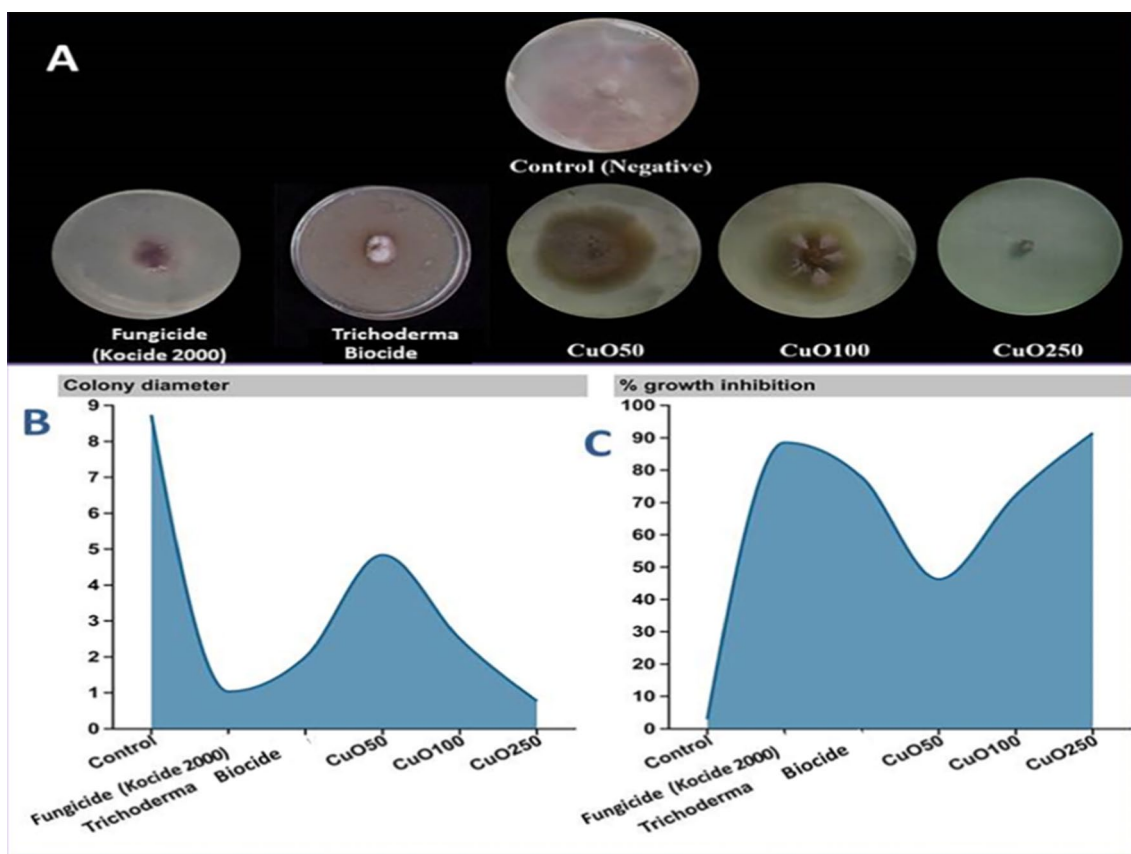


Fig. 4 Antifungal activity of CuO-Zs-NPs at different concentrations as well as a commercial fungicide (Kocide 2000) and Trichoderma biocide against *Fusarium solani* on PDA medium **A:** Inhibitory activity of CuO-Zs-NPs against *F. solani* mycelial growth on PDA medium compared with Trichoderma biocide and the chemical fungicide, **B:** On colony diameter (cm) **C:** On percentage of growth Inhibition (%)

Table 1 Effect of different concentration of CuO-Zs-NPs (50, 100, 250) mg/l, a chemical fungicide and Trichoderma biocide on the mycelial growth and Growth inhibition percentage (%) of *F. solani*

Treatments		Mycelial growth diameter (cm)	Growth inhibition (%)
CuO-Zs-NPs (mg/l)	CuO50	4.83 ± 0.29 ^b	46.30 ± 3.21 ^a
	CuO100	2.5 ± 0.5 ^c	71.36 ± 5.56 ^b
	CuO250	0.77 ± 0.12 ^d	91.17 ± 1.28 ^c
Trichoderma Biocide		2 ± 0.53 ^{bc}	77.09 ± 5.88 ^b
Chemical Fungicide (Kocide 2000)		1.03 ± 0.32 ^d	88.20 ± 3.57 ^a
Untreated Control		9 ± 0.0 ^a	0 ± 0 ^d

Letters on mean values statistically significant differences between the mean of the representative control and the treatments at the same time ($p \leq 0.01$)

CuO-NPs inhibited mycelial FOL growth to 67.3%, compared to 15.6% for a commercial fungicide based on copper hydroxide, making them beneficial against various microbial pathogens that attack plants. Additionally, this would considerably help lower the risk of exposure to

dangerous chemical fungicides, Furthermore, this would significantly contribute to reducing the hazardous effects of toxic chemical fungicides, especially on edible plants and fresh vegetables such as tomatoes [17, 41]. Taken together, our findings support that CuO-Zs-NPs are considered a promising replacement for traditional fungicides in crop protection.

Phytotoxicity test

Impact of CuO-Zs-NPs on the germination of tomato seeds

The effects of different concentrations of CuO-Zs-NPs and its bulk counterpart (fungicide) in compared with Trichoderma biocide on seed germination and seedling length of tomato seeds were evaluated in vitro. The percentages of germination and germination index of tomato seeds treated with 50, 100, and 250 µg/ml CuO-Zs NPs compared to untreated control seeds are shown in Fig. 5.

The data presented in Fig. 5 indicates that all CuO-Zs-NPs treatments considerably had an inductive impact on seed germination ranging from 97.02 ± 1.53–98.67 ± 1.53

in compared to untreated control seeds giving values " 97.07 ± 1.54 . Although treatments with the chemical fungicide and *Trichoderma* Biocide gave higher inductive values (98.33 ± 0.00 , 98.0 ± 1.15) respectively for tomato seed germination, CuO-Zs-NPs at 250 mg/l showed the highest inductive impact on seed germination compared to other treatments. The results also indicated that the addition of CuO-Zs-NPs particularly at 100 and 250 $\mu\text{g}/\text{mL}$ did not negatively affect the number of germinated seeds compared to their bulk counterparts. Although treatment with *Trichoderma* Biocide showed a better effect on seed germination than treatment with CuO-Zs-NPs at 50 $\mu\text{g}/\text{mL}$.

Effect of CuO-Zs-NPs treatments on seed germination and growth vigor

At the 3–5 leaf stage, the effect of CuO-Zs- NPs at concentrations (50, 100, and 250) mg/l on the percentage of tomato seed germination in soil medium was also evaluated and compared individually with the treatment of their counterpart (commercial chemical fungicide Kocide 2000) and *Trichoderma* Biocide (Fig. 5A). The

results indicated that all treatments had no significant stimulating effect on seed germination compared to the untreated control. On the other hand, the results also indicate that the addition of CuO-Zs-NPs particularly at 100 and 50 $\mu\text{g}/\text{mL}$ did not negatively affect the number of germinated seeds compared to their bulk counterparts. Similarly, the unique inductive effect of CuO-Zs-NPs particularly at 100 mg/l was also noticed in other tomato growth parameters such as seedling height, tomato root growth, and the vigor index (Figs. 5(B-D), and 6). A significant, dose-dependent impact on seedling height, root length, and Seedling vigor index was observed in all treatments with CuO-Zs-NPs compared to treatment with either *Trichoderma* biocide or the kocide fungicide (Fig. 5B–D). More interestingly treatments with CuO-Zs-NPs showed a more inductive effect on root length and seedling growth, in contrast to their bulk counterpart which showed a noticeable detrimental effect (Fig. 5). These data were confirmed by Pradhan et al. [66] tested Cu NPs on mung beans, and found that Cu-NPs stimulated plant growth better than copper sulfate. In contrast, Bakshi and Kumar [8] evaluated the effect of Cu-NPs on

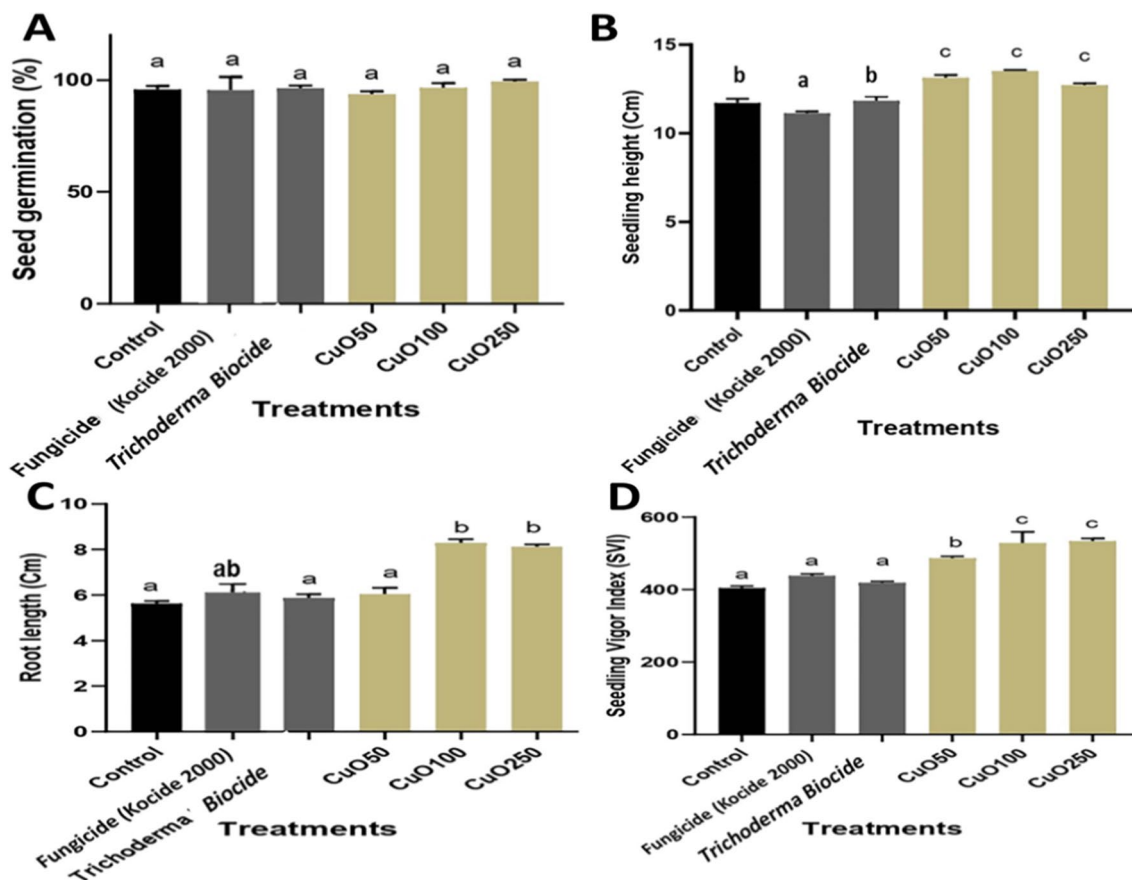


Fig. 5 Effect of CuO-Zs-NPs 50, CuO-Zs-NPs 100, and CuO-Zs-NPs 250, the chemical fungicide “Kocide 2000” and *Trichoderma* biocide on **A** seed germination %, **B** seedling height, **C** Root length, and **D** seedling vigor index of tomato plants

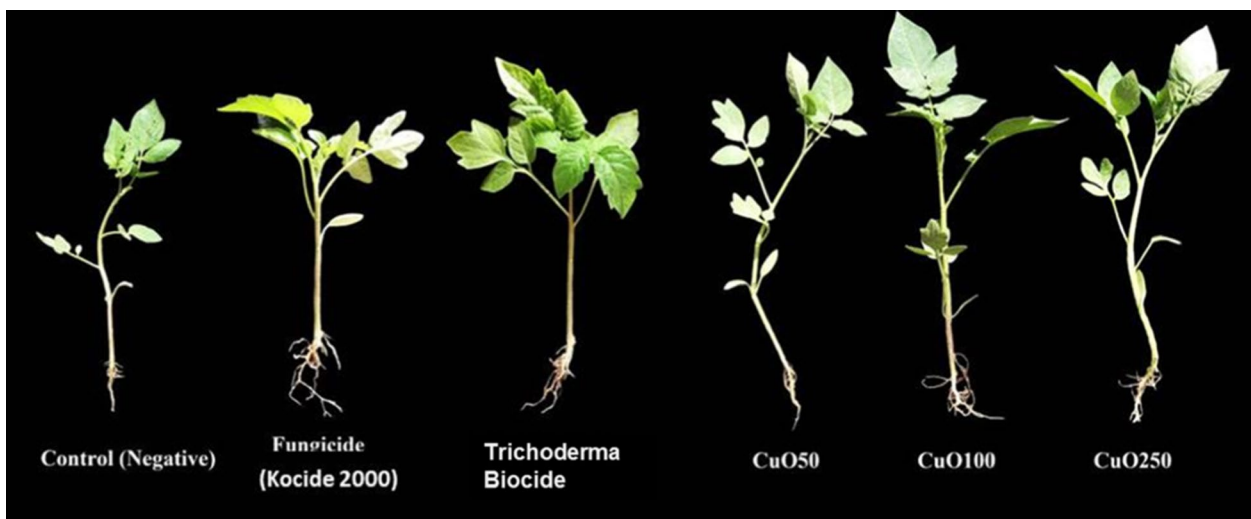


Fig. 6 Effect of CuO-Zs-NPs 50, CuO-Zs-NPs 100, and CuO-Zs-NPs 250, the chemical fungicide "Kocide 2000" and Trichoderma biocide on tomato seedling growth

oregano, and reported that the negative or positive effects of nanoparticles depend on the plant type, nanoparticle concentration, and Cu oxidation state (Fig. 6).

Effectiveness of CuO-Zs-NPs against Fusarium root rot disease infecting tomato plants

The antifungal activity of CuO-Zs-NPs at three different concentrations (Cu50, Cu 100, Cu250) was further investigated in vivo experiment conducted to determine the efficacy of the treatment in controlling Fusarium root rot that affects tomato plants (Fig. 7). Disease severity was recorded for 90 days post inoculation (dpi) in all treated tomato plants. As a comparison, the experiment included plants treated with Kocide 2000 copper fungicide and Trichoderma biocide as chemical and biocide commercial controls respectively.

As early as 15 days post-inoculation, disease signs in mock-treated tomato plants were evident and the plants were visibly weakened; in contrast, disease symptoms in tomato-treated plants were minimal and greatly delayed. Control treatments of tomato plants either with an equivalent chemical fungicide, Kocide 2000, or Trichoderma Biocide also delayed and reduced disease symptoms, but to a lesser extent than CuO-Zs-NPs. A significant reduction in Fusarium root rot disease was noticed for all concentrations of CuO-Zs-NPs compared to the control treated with the pathogen only (infected control) (80.5%). No substantial difference was observed in the disease severity percentage in plants exposed to 50 or 100 mg/l CuO-Zs-NPs. Although treatments with either the chemical fungicide (Kocide fungicide) showed better

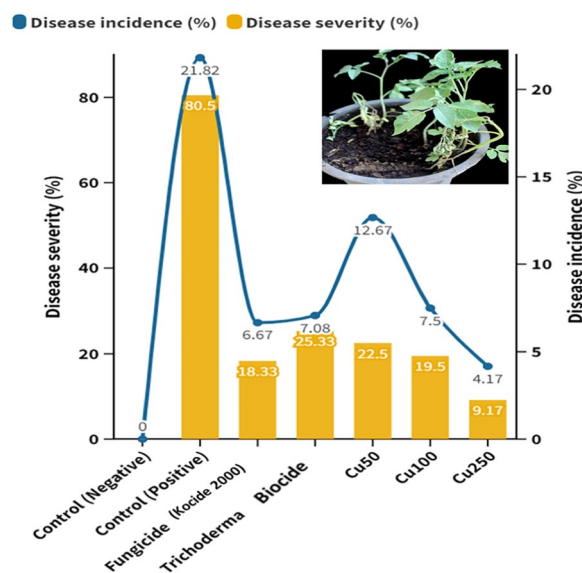


Fig. 7 Disease incidence and severity of Fusarium root rot on infected tomato plants after treatment with CuO-Zs-NPs at (50, 100, 250) mg/L, chemical fungicide, and Trichoderma biocide compared to the positive and negative controls

disease reduction and disease incidence with values of 18.33% and 6.67% respectively, than CuO-Zs-NPs at a concentration of 50 mg/l, however, CuO-Zs-NPs at a dose of 250 mg/l achieved the highest disease reduction (9.17 ± 2.89%) and lowest disease incidence (4.17 ± 3.80%).

Growth and Physiological parameters

Effect on plant height, weight, and chlorophyll content

Three months after seeding, the effects of CuO-Zs-NPs on tomato seedlings were examined for plant lengths, fresh and dry weights, and weight of the resulting fruit (Fig. 8). The results indicated that all CuO-Zs-NPs had a promoting effect on the plant height and tomato (fresh, dry, fruit) weight. In this regard, CuO-Zs-NPs at (50, 100, and 250) mg/l concentration showed an inductive effect on tomato plant height with values 57.67 ± 12.5 , 62.33 ± 7.37 , and 65.33 ± 12.32 respectively, compared to 54.67 ± 3.05 , 55.67 ± 3.51 , and 37 ± 2.65 for treatment with Kocide 2000 fungicide, Trichoderma biocide, and the negative control respectively (Fig. 9). Similarly, the unique inductive effect of CuO-Zs-NPs, particularly at 250 mg/l, was also noticed in data reported for tomato fresh weight, dry weight, and fruit weight. Overall, our data indicate the effectiveness of Cu-Zs-NPs in reducing the disease severity and increasing all growth parameters

and production, which was confirmed by Hernández-Hernández et al. [34]. In addition, the increase in dry weight may be a result of the NPs boosting the activity of photosystems I, II (PSI and PSII), along with the redox state of plastoquinone in the electron transport chain [79].

To investigate the effect of different concentrations of CuO-Zs-NPs on chlorophyll concentration and composition in tomato plant leaves. The total chlorophyll concentration in the control of tomato plant leaves was 0.36 ± 0.014 mg /g fresh weight, whereas, in CuO-Zs-NPs (250, 100 and 50, respectively), it was 0.68, 0.61, and 0.57. However, the composition of chl was significantly different, as evidenced by a decrease in the chl a/b ratio in CuO-Zs-NPs 250 (0.56), this ratio was increased when decreasing the concentration of CuO-Zs-NPs treatment compared to the negative control (0.60) (Fig. 10). While the chl a/b ratio increased in both the biotreatment and the Cu fungicide treatment to 0.66 and 0.67, respectively,

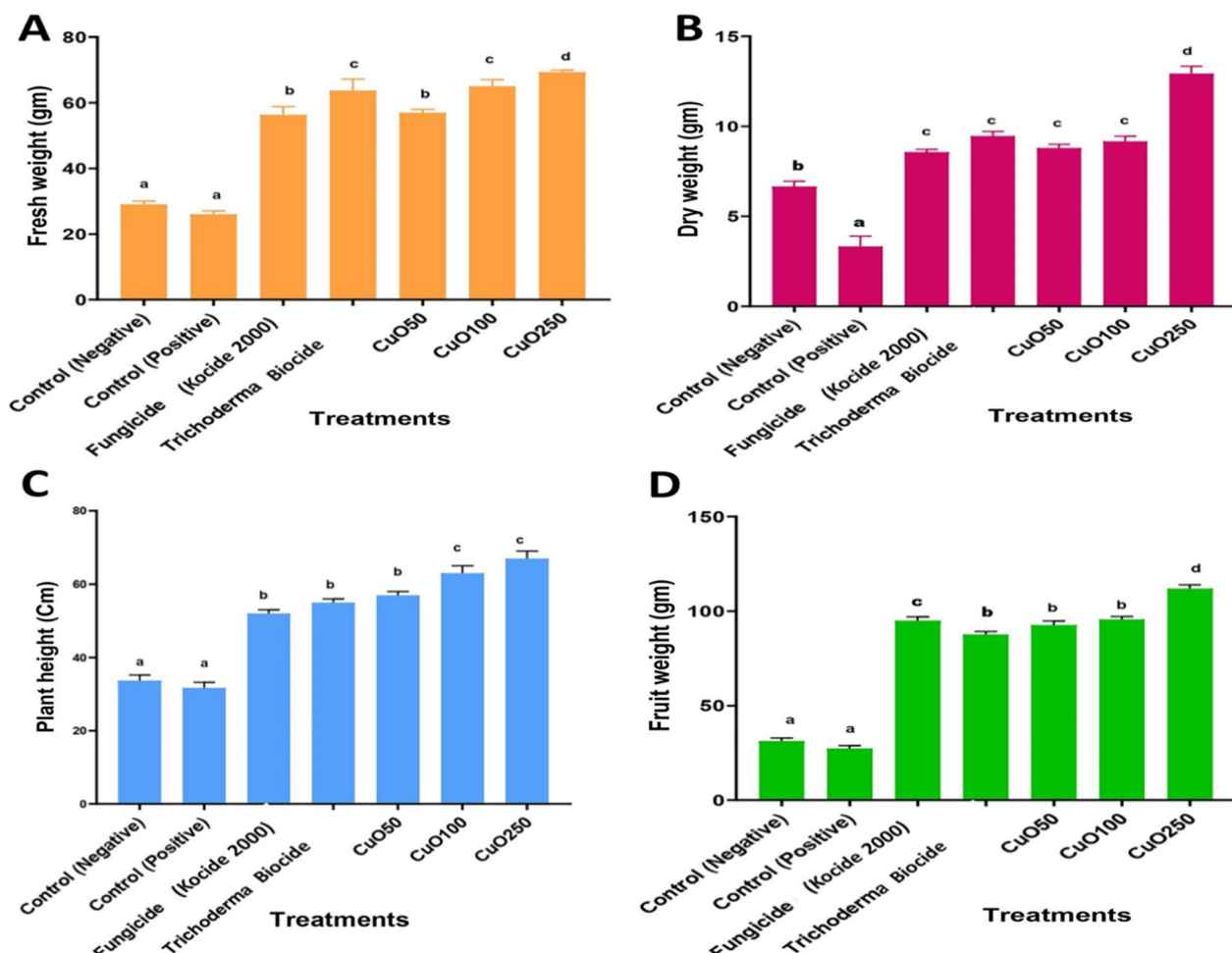


Fig. 8 Effect of different concentrations of CuO-Zs-NPs (50, 100, 250 mg/L), the chemical fungicide "Kocide 2000" and Trichoderma biocide on **A** Fresh weight, **B** Dry weight, **C** Plant height, and **D** Fruit weight of tomato plants challenged with *F. solani*

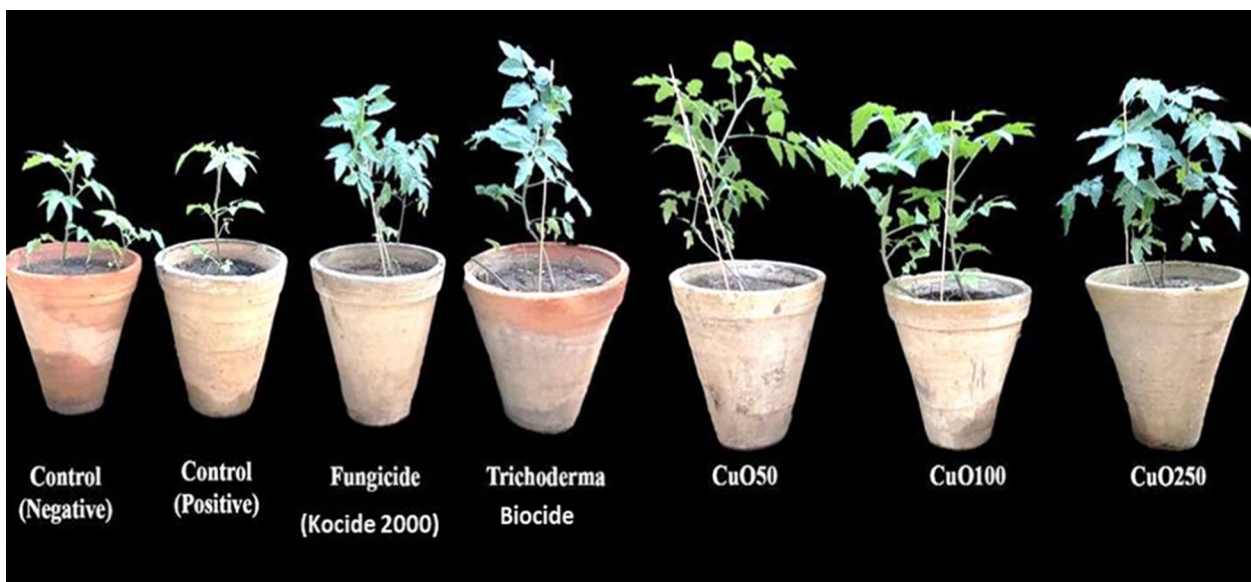


Fig. 9 Effect of different concentrations of CuO-Zs-NPs (50, 100, 250 mg/L), the chemical fungicide "Kocide 2000" and Trichoderma biocide on tomato plants grown in pot experiments treated with *F. solani* compared with the control groups

and both the control and CuO-Zs-NPs 50 had similar cha/chb values.

The enhanced photosystem activity observed in plants exposed to nanoparticles (NPs) may be attributed to the up-regulation of genes related to photosynthesis, such as *psaA* (photosystem, I P700chlorophyll an apoprotein A1), *pet A* (photosynthetic electron transfer A), *HSP90.1* (heat chock protein1), and *psbA* (photosystem, II reaction center protein A) [84]. Additionally, NPs may form complexes with light-harvesting complex (LHC) proteins in the antennae of photosystems, thereby improving light absorption [85]. Furthermore, NPs can increase CO₂ assimilation by enhancing the activity of beta-carbonic anhydrase (BCA) and Rubisco enzymes in light-independent reactions [42, 43]. The promotion of photosynthetic activity by NPs is also responsible for the increased fresh and dry biomass of tomato plants compared to chemical fungicides or Trichoderma biocides. This effect is due to NPs increasing light absorption, accelerating energy transport between photosystems, promoting photolysis of water, and facilitating oxygen evolution [43]. Moreover, the results revealed a significant increase in chlorophyll a (ch-a), b (ch-b), and total chlorophyll content in tomato plants treated with CuO-Zs-NPs compared to other treatments. The concentration of CuO-Zs-NPs had significant effects on chlorophyll content (Fig. 10), with CuO100 and 250 inducing an increase of approximately 50% in chlorophyll a and about 40% in chlorophyll b compared to the control. Similarly, CuO50 also

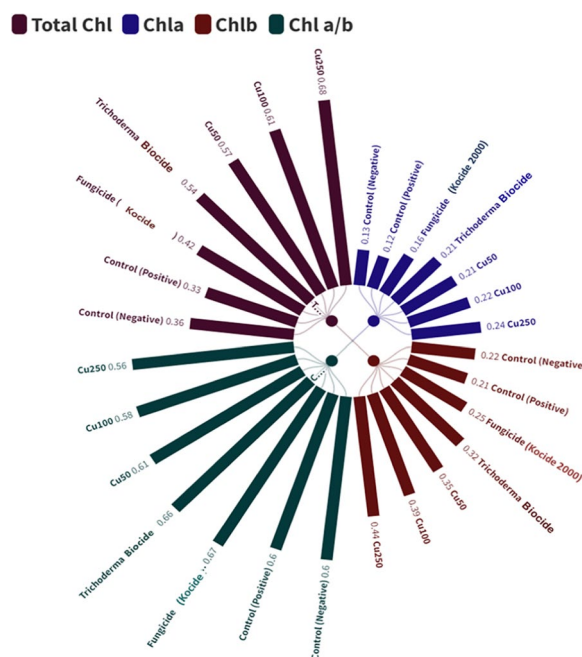


Fig. 10 Effect of different concentrations of CuO-Zs-NPs (50, 100, 250 mg/L), the chemical fungicide "Kocide 2000" and Trichoderma biocide on Chlorophyll a, b, total chlorophyll and Chl a/b ratio of tomato plants treated with *F. solani*

resulted in a moderate increase in chlorophyll a and b, albeit with a relatively smaller amount. All treatments showed an increase in chlorophyll b content, but tomato plants treated with either CuO50, CuO100, or

CuO250 showed significant increases compared to those treated with Kocide 2000 chemical fungicide, biocide, or samples of untreated control. The stimulatory influence of CuO-Zs-NPs on the production of these pigments may be attributed to their ability to enhance plant nutrition by promoting nitrogen absorption. This process can significantly increase the concentration of nutrients in plants, leading to improved growth and increasing phenolic compound concentrations that enhance pigment production [82]. Additionally, the second stage of the bio-stimulation technique for CuO nanoparticles involves the bio-transformation of the core material into ions inside the cytoplasm. Specifically, this process converts CuO nanoparticles into Cu ions. This transformation is likely associated with an increase in chlorophyll levels, which suggests that the ions may be involved in promoting plant growth and photosynthesis. Overall, this second stage of bio-stimulation appears to be an important step in enhancing the effectiveness of CuO nanoparticles for agricultural applications [38]. The increase in chlorophyll a and b concentrations may be explained by the fact that treatments including varied doses of CuO50, CuO100, and CuO250 stimulated strong root development. Where treatments can improve root vitality as in maize, allowing the crop to absorb nutrients from the growing medium [55]. In addition to improving the crop's capacity to absorb light via its photosystems, due to increases in chlorophyll concentrations are thought to be a natural reaction to environmental stimuli [65].

The ratio of chlorophyll a/b is often used as a criterion to estimate crop responses to environmental stresses [78]. Some stresses can cause the conversion of chlorophyll a to b via the enzyme Chl-a oxygenase [13]. The decrease in the Chla/Chlb ratio observed in this study may be due to CuO-Zs-NPs promoting the activity of this enzyme [94]. This results in an increase in Chlb concentration and a reduction in the ratio, indicating a higher concentration of PSII against PSI. This finding is supported by previous research showing that Chlb is abundant in PSII [11, 81]. Increased PSII levels in leaves indicate greater efficiency in absorbing solar energy. Chl-b also plays an important role in arranging thylakoid membranes and regulating LHCs [90]. These results corroborate the earlier descriptions of plant dry matter increase and photosynthetic efficiency.

In conclusion, CuO-Zs-NPs have been found to promote strong root development and increase chlorophyll concentrations in tomato plants. The decrease in the Chla/Chlb ratio observed may be due to the increased activity of the enzyme responsible for synthesizing Chlb from Chla. These findings suggest that CuO-Zs-NPs may have potential applications for improving crop growth and productivity.

Effect of CuO-Zs-NPs on enzymatic activities of treated plants

In the pot experiment, to understand more about the interaction of *F. solani* with tomato plants following the application of CuO-Zs-NPs at varied concentrations. A

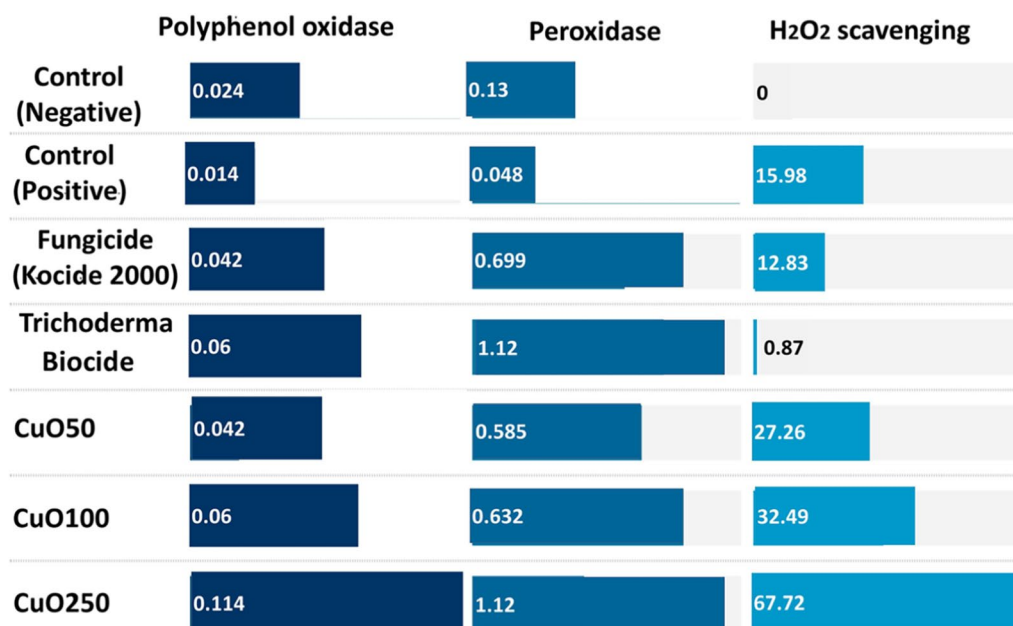


Fig. 11 Effect of CuO-Zs-NPs 50, CuO-Zs-NPs 100, and CuO-Zs-NPs 250, the chemical fungicide “Kocide 2000” and Trichoderma biocide on some enzymatic activity “polyphenol oxidase, Peroxidase, H₂O₂ Scavenging” of tomato plants challenged with *F. solani*

number of defense-related enzymes were examined. The data obtained showed that the inoculation of *F. solani* improved the activity of all the defense-related enzymes examined in all treatments compared to the un-inoculated control plants. The CuO-Zs-NPs significantly modified the enzymatic activity of polyphenol oxidase and peroxidase in tomato leaves (Fig. 11). The interaction of CuO-Zs-NPs at 50, 100, and 250 mg/l increased the activity of the polyphenol oxidase enzyme to 75, 150 and 375% respectively compared to the non-treated healthy and infected tomato plants showing polyphenol oxidase enzymatic activity of 0.024 and 0.014 U/min/gram respectively. In contrast, treatment with the chemical fungicide and Trichoderma Biocide that increased polyphenol oxidase activity to 75, and 150% respectively.

On the other hand, the peroxidase enzyme was increased to 350, 386, and 762% respectively in comparison with the non-treated healthy and infected tomato plants that showed peroxidase enzymatic activity 0.13, 0.048 U/min/gram respectively. In contrast, treatment with the chemical fungicide and Trichoderma Biocide increased peroxidase activity to 415, and 762% respectively. Additionally, the activity of hydrogen peroxide (H_2O_2) scavengers as an antioxidant response to oxidative stress potentially caused by CuO-Zs-NPs treatments was determined in tomato plant leaves. The results indicated that both CuO-Zs-NPs and the chemical fungicide treatments exhibited higher levels of H_2O_2 scavenger activity than the Trichoderma biocide treatment and the untreated control (Fig. 11).

Overall, the results of our study indicate that the application of CuO-Zs-NPs exogenously can enhance the resistance of tomato plants against *F. solani* infection. This finding is consistent with previous reports demonstrating that certain derived compounds, when applied externally, can induce resistance in host plants by elevating the levels of host defense enzymes and pathogen-related (PR) proteins [36]. It is suggested that CuO-Zs-NPs may trigger systemic acquired resistance (SAR) in host plants, thereby reducing their susceptibility to infection, as described previously [36]. SAR is a plant immune response that prevents the spread of infection or disease to non-infected parts of the host plant and is typically characterized by an increase in PR proteins such as chitinases, -1,3-glucanases, acid invertases, and peroxidases [4, 10, 77]. Several studies have shown that substances derived from plants can stimulate the development of more resistant crops and reduce disease incidence [61, 67]. The induction of systemic resistance in plants involves the activation of dormant defense genes under various conditions.

Numerous studies have reported that increased levels of peroxidase, protease, and polyphenol oxidase (POD)

enzyme activity, as well as the expression of genes for -1,3-glucanase and chitinase, are effective against various fungal diseases [61, 67]. This is in line with Fernandes, & Ghag, [25] provided an inclusive assessment of tomato genes involved in pathogen detection, defense signaling networks, and the functions of enzymes that support host resistance to *Fusarium solani*. CuO-Zs-NPs treatments at various concentrations have been shown to increase defense-related enzymes and pathogenesis-related proteins in tomato plants against root rot pathogens. These proteins may play a crucial role in strengthening the host plant's cell walls to resist *F. solani* infection. Additionally, CuO-Zs-NPs may activate defense mechanisms in response to pathogen inoculation by developing additional proteins to prevent pathogen entry or subsequent spread due to the importance of Cu as a microelement for plants. Furthermore, recent studies have also demonstrated the role of Cu Bio-nanoparticles in increasing H_2O_2 scavenger activity as an anti-resistance mechanism against stress or toxicity [87]. The application of Cu nanoparticles has been shown to enhance antioxidant enzyme activity and reduce oxidative damage caused by stress or toxicity. Therefore, it can be concluded that Cu nanoparticles have potential applications in enhancing plant defense mechanisms against various biotic and abiotic stresses.

Determination of Cu content in terminal apical tomato tissues

Tomato crop growth is dependent on a range of essential nutrients, both macronutrients (such as N, P, K, Ca, and Mg) and micronutrients (such as Cu, Fe, B, Mn, and Mo). These nutrients are crucial for various processes including photosynthesis, cellular respiration, and defense responses. The roots are the primary site for nutrient absorption. Cu is particularly important in mitigating Reactive Oxygen Species (ROS), facilitating photosynthesis, regulating phenol metabolism, and promoting protein synthesis [86, 87]. As shown in Table 2, tomato plants treated with the chemical fungicide Kocide 2000, showed the highest conc. of Cu with a 17.244 ± 0.22 value, followed by 12.372 ± 0.22 , 12.516 ± 1.2 , and 15.344 ± 0.32 for CuO-Zs-NPs 50, 100, and 250 treatments respectively, compared to 10.983 ± 0.40 for treatment with Trichoderma biocide and 10.272 ± 0.24 and 10.297 ± 0.35 for negative and positive controls respectively. In view of the obtained results and inconsistent with other research [34], increasing the conc. of Cu particularly at their nanoscale could promote the growth of tomato roots which directly improved seed germination, plant height, and fresh and dry weight as indicated above in (Figs. 5, 8) without any adverse effects. This is in agreement with [54] who reported that exposure of plant leaves to

Table 2 The Cu content in tomato terminal bud tissues after applying the CuO NPs treatments in compared to treatment with the chemical fungicide, Trichoderma biocide and the (positive, negative) controls

Treatment	Cu conc. (mg/l)
CuO50	12.372 ± 0.22 ^b
CuO100	12.516 ± 1.2 ^b
CuO250	15.344 ± 0.32 ^c
Trichoderma biocide	10.983 ± 0.40 ^a
Fungicide (Kocide 2000)	17.244 ± 0.22 ^d
Post. Control	10.297 ± 0.35 ^a
Neg. control	10.272 ± 0.24 ^a

Bars with the same letters are not statistically significant based on the least significant difference (LSD) test ($P < 0.05$)

varying concentrations of Cu NPs did not result in an increase in Cu content in the fruits. However, some studies have suggested that the accumulation of Cu, Fe, Mn, and Zn in leaves may occur through uptake by plants via leaf apertures such as stomata, trichomes, and hydathodes when applied in foliar or through water uptake via root absorption [6]. Micronutrient regulation, particularly Cu, occurs during different pathways of transport that facilitate migration to the needed areas. Ghasemi et al. [23] found that some nutrients may cause fluctuations in other microelements, which can cause them to accumulate in different tissues.

This may explain the accumulation of copper (Cu) in tomato plant leaves when exposed to the fungicide Kocide 2000 at a high concentration of 2.5 g/L, which may not give the best positive effects on some growth and physiological parameters in compared to lower dosages of CuO treatments at the nanoscale as indicated above. These findings suggest that CuO-Zs-NPs nanoparticles can enhance root growth and nutrient absorption, which could be considered another reason for promoting tomato growth in compared to other treatments. Additionally, the use of CuO nanoparticles in soil may mitigate environmental contamination caused by excessive agrochemical use.

Pollen grain analysis

The data in Table (3) indicate that the effect of Cu nanoparticles on the pollen grain fertility of tomato plants was analyzed. The results indicated that treatments with CuO-Zs-NPs at the lowest concentrations led to a rising number of mature pollen grains (Fig. 13M) compared to the immature ones (Figs. 12A and 13L). This is possibly, due to the early flowering of the plants treated with CuO-Zs-NPs. Which can affect the photosynthesis and respiration process of the plants, and influence the production

of sugars and energy that are required for flowering. Similarly, treatment with Trichoderma (biocide) showed a noticeable increase in the number of mature pollen grains compared to the control samples. These findings are in agreement with data obtained by Marmioli et al. [56], who reported that no aspect of the plant's appearance, development, or pollen formation changed after being treated with high concentrations (320 mg/kg⁻¹) of nano-CuO. In contrast, some reports revealed that copper NPs decreased black cumin's fertility, suggesting that these NPs may have acted as a barrier to pollen formation or to the plant's normal development and maturation [48]. Additionally, fertile pollen grains of abnormal size in diploid 2n (Fig. 13O arrow) were observed in compared to normal (n) pollen grains (Fig. 13M), where meiosis was perfectly normal in the control treatment (Fig. 13A, B and E). Fertile n was found to be elevated to 91.5 in CuO-Zs-NPs at a concentration of 50mg/l, approaching the values (99 ± 8.7 of untreated (negative control, and there was no significant difference between them. On the other hand, the obtained results indicated that exposure of tomato tissues to Cu-Zs-NPs, particularly at the highest conc. (250 mg/l inhibited pollen development in the flowering stage. This is also suggested to have an adverse effect on pollen fertility which was recorded (30.1 ± 1.7% for n fertile pollens and (3.1 ± 0.2 for 2n fertile pollens; subsequently, the total fertile pollens for this treatment were recorded (33.22% (Table 3).

While the treatment with biocide recorded (68.7 ± 2.9) for the haploid (n) fertile pollen grain and (3.1 ± 0.2) for the diploid pollen, resulting in a total of 71.88% fertile pollen (Fig. 12B). Then, the chemical fungicide was recorded (49.7 ± 4.1) in haploid pollens and (2.9 ± 0.1) in diploid pollens to enhance the number of total fertile pollens to 52.7%. Additionally, there were slight increases in the 2n% value and no significant difference among the treatments with CuO-Zs-NPs at conc. 100 mg/l (2.4 ± 0.1), the chemical fungicide (2.9 ± 0.1), CuO-Zs-NPs at conc. 250 mg/l (3.1 ± 0.2), and Trichoderma biocide (3.1 ± 0.2). Treatment with *F. solani* only increased the diploid 2n to 11.8%. To explain this, we suggest that the damage caused by *F. solani* to tomato root tissues leads to a functional impairment that occurs from nutritional imbalances, which had the greatest effect on the abnormal appearance [49]. On the other hand, other reports suggest that the effect of CuONPs possibly prevents centromeric division, leading to the production of extra chromosomes (Diplo-chromosomes) [48]. Additionally, polyploid cells and stragglers can be caused by defects in the spindle process.

ANOVA statistical analyses indicated a noticeable significant difference ($P < 0.05$) between most of the

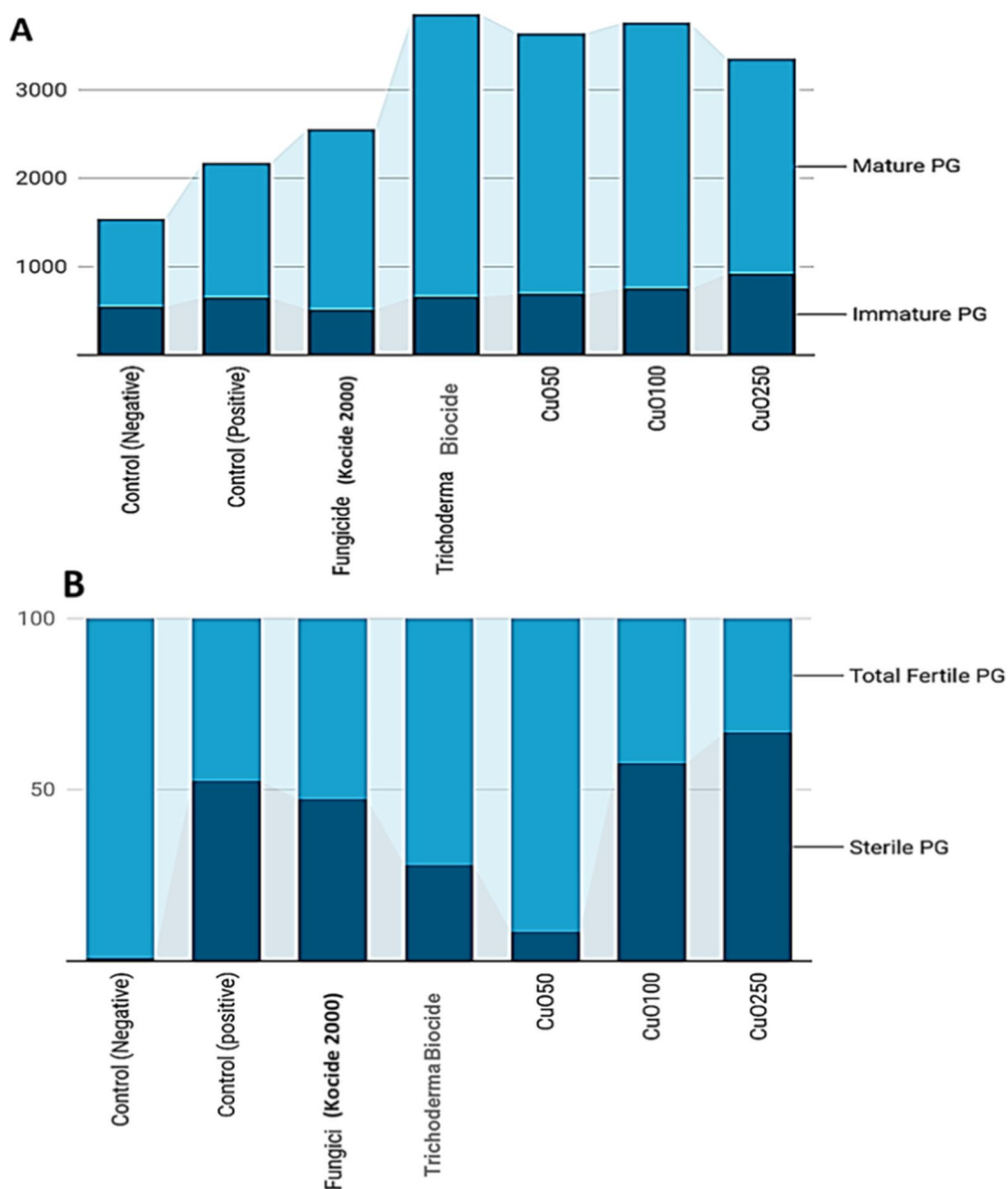


Fig. 12 Effect of different concentration of CuO-Zs-NPs on the percentage (%) of pollen grains maturity (A); and fertility in compared to treatment with the chemical fungicide and Trichoderma biocide (B)

experimental groups compared to the control group of sterile PG (Fig. 13N). However, when comparing the fungicide-positive control with the copper-based Cu 100, there was no statistically significant difference ($P > 0.05$) (Table 3). The results indicated a noticeable sterile pollens (unstained pollens, Fig. 13N) which increased significantly in the treatment with CuO-Zs-NPs at conc. 250 mg/l, which was 66.8 ± 5.6 , but there was no significant difference between the treatment with CuO-Zs-NPs at conc. 100 mg/l, 57.7 ± 2.2 , and the positive control, 52.6 ± 0.7 . On the other hand, the biocide treatment

recorded a moderate rate (28.1 ± 2.8). The results also showed no significant difference between the positive control and the treatment with the chemical fungicide (47.3 ± 1.6). While the best treatment was CuO-Zs-NPs at a concentration of 50 mg/l giving (8.5 ± 0.2), where there was no noticeable significant difference with the negative control (1 ± 0.2).

Although treatments with CuO-Zs-NPs (100, 250 mg/l), and the chemical fungicide decreased the passive effect of *E. solani* on the tomato host plant, the treatments increased the negative effect (sterility) on pollen

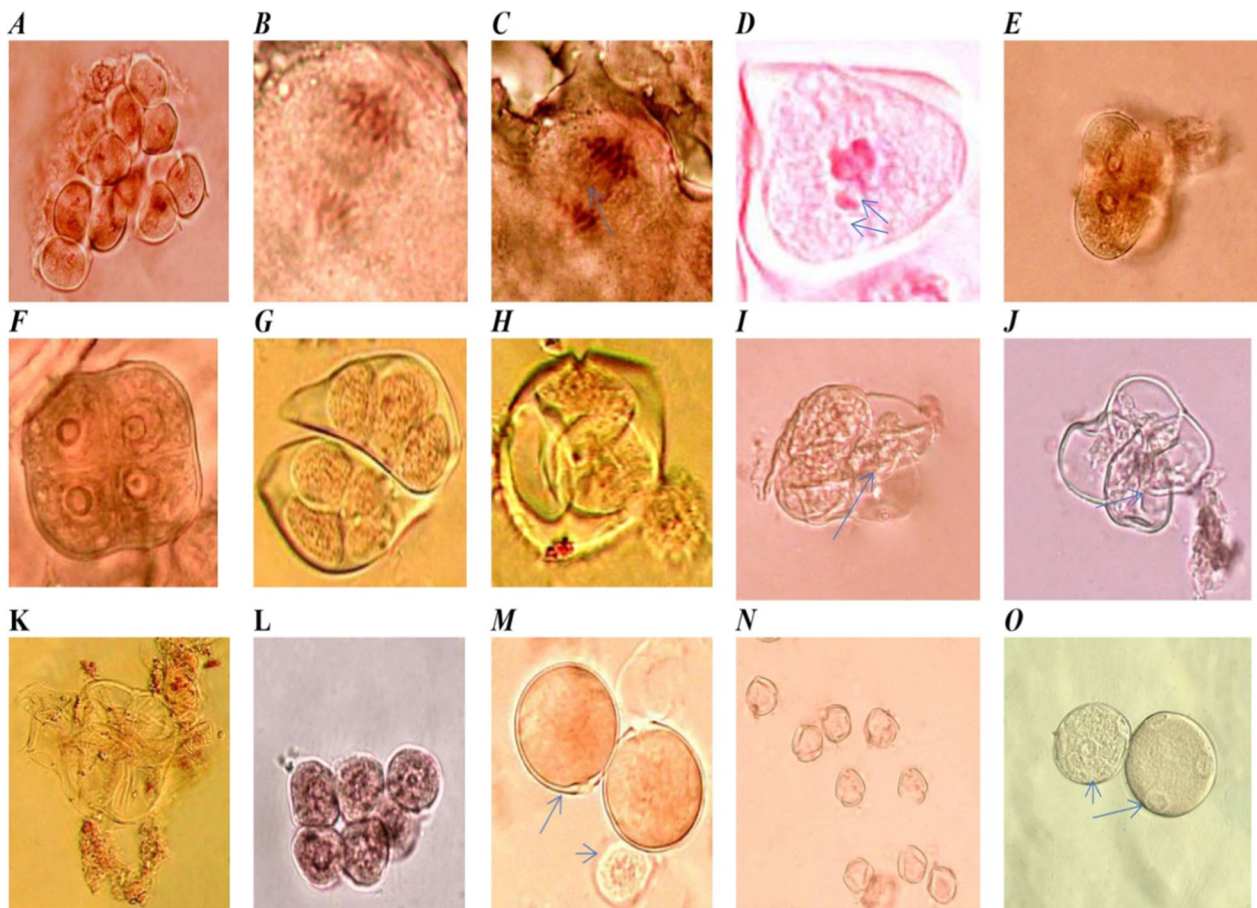


Fig. 13 **A.** Divided cell in meiosis I and II; **B.** Normal anaphase I; **C.** Anaphase I with lagging chromosome arrow; **D.** Metaphase I with lagging chromosome and fragment arrow **E.** Diad pollen grain arrangements; **F.** Normal Microspore tetrad (isobilateral); **G.** Normal Microspore tetrad (Liner and Decussate) **H.** Tetrad release immature PG arrowhead (Tetrahedral); **I.** Two cells from tetrad lose cytoplasmic granules arrows; **J.** All cells formed tetrad lose cytoplasmic granules; **K.** cytoplasmic granules outside tetrad arrows; **L.** immature PGs; **M.** Mature Fertile PGs (reduce) arrow and immature arrowhead; **N.** Sterile PGs; **O.** Mature fertile 2n pollen grain arrow (unreduced)

Table 3 Effect of CuO-Zs-NPs treatments at the three different concentrations (50, 100, and 250) mg/l on the percentage (%) of pollen grain fertility in compared to the chemical fungicide and Trichoderma biocide treatments

Treatments	N of Tetrad	N of Immature PG	Total N mature PG	Sterile PG %*	Fertile PG		
					n%*	2n%*	Total fertile
CuO50	70	689	2950	8.5 ± 0.2 ^E	91.5 ± 0.3 ^A	0 ± 0 ^C	91.53
CuO100	75	750	3008	57.7 ± 2.2 ^B	39.8 ± 2.0 ^{CD}	2.4 ± 0.1 ^B	42.31
CuO250	110	915	2435	66.8 ± 5.6 ^A	30.1 ± 1.7 ^D	3.1 ± 0.2 ^B	33.22
Trichoderma biocide	50	655	3200	28.1 ± 2.8 ^D	68.7 ± 2.9 ^B	3.1 ± 0.2 ^B	71.88
Fungicide	150	514	2040	47.3 ± 1.6 ^C	49.7 ± 4.1 ^C	2.9 ± 0.1 ^B	52.7
Positive Control	100	650	1520	52.6 ± 0.7 ^{BC}	35.6 ± 0.1 ^{CD}	11.8 ± 0.4 ^A	47.43
Untreated Control (Negative)	212	544	1000	1 ± 0.2 ^E	99 ± 8.7 ^A	0 ± 0 ^C	99

N: number, n, haploid. 2n diploid*% percentage from total mature PG; Bars with the same letters are not statistically significant based on the least significant difference (LSD) test ($P < 0.05$)

grains resulting in chromosomal lagging and fragments that induced mutations (Fig. 13C, and D). The decrease in the proportion of viable pollen grains in these treated plants relative to untreated plants can be attributable to their pollen-toxic effects. In fact, this harmful effect becomes more apparent when fungicides and high concentrations of CuO-Zs-NPs are used. Sterility occurs during the formation of gametophytes, most likely initiating at the microspore stage, and gametophytes are aborted at the beginning of their development. These findings are contrary to data obtained by Marmiroli et al. [56], who reported no changes in the development or viability of pollen after treatment with high concentrations (320 mg/kg) of nano-CuO.

The diploid gametes (Fig. 13O) may result from a variety of cytological abnormalities due to the five main cytological mechanisms of $2n$ gamete formation: pre-meiotic chromosome doubling during the transition from mitosis to meiosis, meiosis disturbances, and abnormal cytokinesis during the first or second meiosis resulting in dyad and triad formation (Fig. 13E, H), followed by $2n$ pollen formation. In this regard, some studies estimated the frequency of $2n$ pollen grains and suggested that they came from restoration nuclei generated during meiosis I and II as dyads and triads in the spore stage (Xue, Liu, and Liu [92]). Large-sized $2n$ pollen grains were observed to be well-filled, pigmented, and viable; hence, it is highly probable that fertilization by these $2n$ gametes can result in intraspecific polyploidy. Additionally, Sabrine et al., [74] mentioned that higher Cu concentrations disrupt critical functions such as mitosis and photosynthesis, causing plant tissue toxicity [70, 74]. Furthermore, heavy metals disrupt the mitotic cycle, cause chromosomal aberrations, microtubule damage, irregularly shaped nuclei, and decompose nuclear material [91], Eun, Shik Youn, and Lee [22]).

The results recorded a clear observation in the frequency pattern of a normal tetrad (isobilateral) and tetrads linear and Decussate (Fig. 13F, G) in comparison to that in the case of the frequency pattern of tetrad release immature PG (Tetrahedral), which showed that treatment with CuO-Zs NPs results in a clear observed loss of cytoplasmic granules in tetrad cells either outside or inside cells (Fig. 13H–K), such as the non-disjunction of chromosomes in both meiotic divisions. These findings can be explained by manipulations in male meiosis as indicated in Berdnikov et al [9]. Additionally, the treatments induce structural damage to the cell in the tetrad-stage pollen cytoplasm Grain (PCG) are naturally released from the pollen grain when the cytoplasm is expelled from the pollen grains through the pore. However, release could also occur through cracks of the exine when the pollen was damaged. Only a small proportion

of the pollen releases their cytoplasm, and the remaining pollen remains intact. However, in fragile pollen, PCG release can also occur through breaks of the exine cytoplasmic granules that can be seen next to the pollens that come out of them. Our results showed that cytoplasmic granules were expelled from the cells in tetrad stages. Tetrad cytoplasmic granules can be seen next to tetrad stage also. Furthermore, the tetrads with two deadly pollen grains may result primarily from non-disjunction in anaphase I, and those with one pollen grain may result primarily from non-disjunction in anaphase II [9]. This phenomenon results from the interaction of cell division and pollen development with some toxic treatments and increases the proportion of cytoplasmic granules released. These reasons also decreased the final percentage of total fertile pollen grains in the treated plants compared with the control, which can be attributed to their toxic effect on pollen.

Conclusions

The present study explores the usage of *Ziziphus spina-Christi* wild leaf extract in green chemistry to synthesize copper oxide nanoparticles (CuO-Zs-NPs) for combating *Fusarium solani* that causes root rot on tomato plants. The results indicated that CuO-Zs-NPs exhibited superior activity in both laboratory and greenhouse experiments against *Fusarium* root rot more effectively than both commercial fungicides “Kocide 2000” and Biocide (*Trichoderma viride* 1.5% W.P) under in vitro and in vivo conditions. Interestingly, Cu concentration was higher in tomato plants treated with chemical fungicides compared to CuO-Zs-NPs, but at their nano scale, they significantly enhanced nutrient absorption, root growth, improving seed germination, plant height, fresh and dry weight, photosynthetic and enzymatic parameters. Treatment with *Trichoderma* Biocide and CuO-Zs-NPs at low concentrations led to a rise in mature pollen grains, but at high concentrations, it increased the percentage of sterile PG and induced Tetrad cytoplasmic granules. The unique antifungal properties of CuO-Zs-NPs make them a promising bio-nanomaterial for crop protection strategies and could replace synthetic fungicides as safer alternatives. However, further research is still needed to fully understand the structure-activity relationship of CuO-Zs-NPs, scale up their synthesis procedure, and produce stable formulations with desirable characteristics.

Acknowledgements

The first author would like to thank Dr. Yousra H. Kotp and all the members of “Water Treatment & Desalination Unit, Hydrogeochemistry Department, Desert Research Center” due to their support during the study.

Author contributions

The study’s design was motivated by Sozan El-Abeid and Mohamed A. M. El-Tabakh. Nanomaterials synthesis and characterization were conducted

by S. El-Abeid. Both in vitro and in vivo investigations were performed by Mohamed A. Mosa and S. El-Abeid. Acquired molecular fungal identification and sequencing analysis were performed by S. E. El-Abeid; Mohamed A.M. El-Tabakh and Mohamed A. Mosa. Maha S. A. Haridy made the pollen grain sterile and a fertile analysis test. while sample collection was made by Mohamed A. El-Khateeb; Maha S. A. Haridy and A. M. Saleh. Data analysis was done by all contributors. S. El-Abeid and Mohamed A. Mosa wrote and reviewed the manuscript. All authors have reviewed and agreed to the published version of the manuscript.

Funding

Open access funding provided by The Science, Technology & Innovation Funding Authority (STDF) in cooperation with The Egyptian Knowledge Bank (EKB). All authors declare that "No fund received to carry out this work."

Availability of data and materials

The datasets generated and/or analyzed during the current study are available in within the article.

Declarations

Ethics approval and consent to participate

Not applicable.

Consent for publication

Not applicable.

Competing interests

All authors declare that they have no competing interests.

Author details

¹Nanotechnology & Advanced Nano-Materials Laboratory (NANML), Plant Pathology Research Institute, Agricultural Research Center, Giza 12619, Egypt. ²Mycology and Disease Survey Research Department, Plant Pathology Research Institute, Agricultural Research Center, Giza 12619, Egypt. ³Zoology Department, Faculty of Science, Al-Azhar University, Cairo, Egypt. ⁴Department of Pharmaceutical Chemistry, Faculty of Pharmacy, Horus University, Horus 34518, Egypt. ⁵Water Pollution Research Dep, National Research Centre, Dokki, Cairo, Egypt. ⁶Central Lab of Organic Agriculture, Agricultural Research Center (ARC), 9 Gamaa St, Giza 12619, Egypt.

Received: 4 August 2023 Accepted: 19 December 2023

Published: 12 January 2024

References

- Abboud Y, Saffaj T, Chagraoui A, El Bouari A, Brouzi K, Tanane O, Hssane B. Biosynthesis, characterization and antimicrobial activity of copper oxide nanoparticles (CONPs) produced using brown alga extract (*Bifurcaria bifurcata*). *Appl Nanosci*. 2014;4:571–6.
- Afkhami A, Moosavi R. Adsorptive removal of Congo red, a carcinogenic textile dye, from aqueous solutions by maghemite nanoparticles. *J Hazard Mater*. 2010;174:398–403.
- Akanbi-Gada MA, Ogunkunle CO, Vishwakarma V, Viswanathan K, Fatoba PO. Phytotoxicity of nano-zinc oxide to tomato plant (*Solanum lycopersicum* L.): Zn uptake, stress enzymes response and influence on non-enzymatic antioxidants in fruits. *Environ Technol Innov*. 2019;14:100325.
- Ali S, Mir ZA, Bhat JA, Anshika Tyagi N, Chandrashekar PY, Rawat S, Sultana M, Grover A. Isolation and characterization of systemic acquired resistance marker gene PR1 and its promoter from *Brassica juncea*. *3 Biotech*. 2018;8:1–14.
- Ansilin S, Kavya Nair J, Aswathy C, Rama V, Peter J, Jeyachinthaya J, Persis. Green synthesis and characterisation of copper oxide nanoparticles using *Azadirachta indica* (Neem) leaf aqueous extract. *J Nanosci Technol*. 2016;31:221–3.
- Avellan A, Yun J, Morais BP, Clement ET, Rodrigues SM, Lowry GV. Critical review: Role of inorganic nanoparticle properties on their foliar uptake and in planta translocation. *Environ Sci Technol*. 2021;55:13417–31.
- Bailey RA. A unified approach to design of experiments. *J Royal Statist Soc Series A*. 1981;144:214–23.
- Bakshi M, Kumar A. Copper-based nanoparticles in the soil-plant environment: Assessing their applications, interactions, fate and toxicity. *Chemosphere*. 2021;281: 130940.
- Berdnikov VA, Kosterin OE, Bogdanova VS. Mortality of pollen grains may result from errors of meiosis: study of pollen tetrads in *Typha latifolia* L. *Heredity*. 2002;89:358–62.
- Butt UR, Naz R, Nosheen A, Yasmin H, Keyani R, Hussain I, Hassan MN. Changes in pathogenesis-related gene expression in response to bioformulations in the apoplast of maize leaves against *Fusarium oxysporum*. *J Plant Interact*. 2019;14:61–72.
- Caffarri S, Tibiletti T, Jennings RC, Santabarbara S. A comparison between plant photosystem I and photosystem II architecture and functioning. *Curr Protein Pept Sci*. 2014;15:296–331.
- Chandraker SK, Ghosh MK, Lal M, Ghorai TK, Shukla R. Colorimetric sensing of Fe³⁺ and Hg²⁺ and photocatalytic activity of green synthesized silver nanoparticles from the leaf extract of *Sonchus arvensis* L. *New J Chem*. 2019;43:18175–83.
- Chen Y, Gao X. Comparison of two methods for phytoplankton chlorophyll-a concentration measurement. *J Lake Sci*. 2000;12:186–8.
- Chen Yu, Jinying Lu, Liu M, Li H, Sun Q, Nechitaylo GS, Bogoslovskaya OA, Olkhovskaya IP, Glushchenko NN. Tomato response to metal nanoparticles introduction into the nutrient medium. *IET Nanobiotechnol*. 2020;14:382–8.
- Çolak A, Biçici M. PCR detection of *Fusarium oxysporum* f. sp. *radicis-lycopersici* and races of *F. oxysporum* f. sp. *lycopersici* of tomato in protected tomato-growing areas of the eastern Mediterranean region of Turkey. *Turk J Agric For*. 2013;37:457–67.
- Coleman JJ. The *Fusarium solani* species complex: ubiquitous pathogens of agricultural importance. *Mol Plant Pathol*. 2016;17:146–58.
- Dreyer DR, Ruoff RS, Bielawski CW. From conception to realization: an historical account of graphene and some perspectives for its future. *Angew Chem Int Ed*. 2010;49:9336–44.
- El-Abeid SE, Ahmed Y, Daròs J-A, Mohamed MA. Reduced graphene oxide nanosheet-decorated copper oxide nanoparticles: a potent antifungal nanocomposite against *Fusarium* root rot and wilt diseases of tomato and pepper plants. *Nanomaterials*. 2020;10:1001.
- Elagamey E, Abdellatef MAE, Haridy MSA, Abd E-S, El-aziz. Evaluation of natural products and chemical compounds to improve the control strategy against cucumber powdery mildew. *Eur J Plant Pathol*. 2023;165:385–400.
- Elshahawy I, Abouelnasr HM, Lashin SM, Darwesh OM. First report of *Pythium aphanidermatum* infecting tomato in Egypt and its control using biogenic silver nanoparticles. *J Plant Prot Res*. 2018;58(2):137–151.
- Eswaran A, Muthukrishnan S, Mari KR, Manogaran P. Phytochemical analysis and free radical scavenging activity of green-synthesized *dlv-pro-08* formulation. *RJLBPCS*. 2019;5:613–25.
- Eun S-O, Youn HS, Lee Y. Lead disturbs microtubule organization in the root meristem of *Zea mays*. *Physiol Plant*. 2000;110:357–65.
- Faghihi-Sani M, Ghasemi H, Kokabi A, Riazi Z. Alumina-copper eutectic bond strength: contribution of preoxidation, cuprous oxides particles and pores. *Scientia Iranica*. 2009;16(3): 263–268.
- FAO. Production/crops and resource/fertilizer. Rome, Italy: FAOSTAT Database Collections. 2019.
- Fernandes LB, Ghag SB. Molecular insights into the jasmonate signaling and associated defense responses against wilt caused by *Fusarium oxysporum*. *Plant Physiol Biochem*. 2022;174:22–34.
- Ghavam M, Bacchetta G, Castangia I, Manca ML. Evaluation of the composition and antimicrobial activities of essential oils from four species of *Lamiaceae* Martinov native to Iran. *Sci Rep*. 2022;12:17044.
- Ghidan AY, Al-Antary TM, Awwad AM. Green synthesis of copper oxide nanoparticles using *Punica granatum* peels extract: effect on green peach Aphid. *Environ Nanotechnol Monitoring Manag*. 2016;6:95–8.
- Ghorai TK, Pathak S, Sikdar S. Synthesis, characterization and environmental applications: using metal-niobium-titanate $M \times Nb \times Ti_{1-2x} O_{2-x/2}$ ($M = Cr, Fe$; $x = 0.01-0.2$) Nano-Composites. *Adv Sci Lett*. 2016;22:167–74.

29. Gong Y, Toivonen PMA, Lau OL, Wiersma PA. Antioxidant system level in 'Braeburn' apple is related to its browning disorder. *Bot Bull Acad Sin.* 2001;42:259–264.
30. Gorin N, Heidema FT. Peroxidase activity in Golden Delicious apples as a possible parameter of ripening and senescence. *J Agric Food Chem.* 1976;24:200–1.
31. Goyal S, Shaharun MS, Kait CF, Abdullah B, Ameen M. Photoreduction of carbon dioxide to methanol over copper based zeolitic imidazolate framework-8: a new generation photocatalyst. *Catalysts.* 2018;8:581.
32. Hamza A, Mohamed A, Derbalah A. Unconventional alternatives for control of tomato root rot caused by *Rhizoctonia solani* under greenhouse conditions. *J Plant Prot Res.* 2016;56(3):298–305.
33. Haridy MH, El-Said MAA. Estimates of genetic parameters using populations in faba bean (*Vicia faba* L.). *J Plant Prod.* 2016;7:1443–7.
34. Hernández HH, Benavides-Mendoza A, Ortega-Ortiz H, Hernández-Fuentes AD, Juárez-Maldonado A. Cu Nanoparticles in chitosan-PVA hydrogels as promoters of growth, productivity and fruit quality in tomato. *Emirates J Food and Agric.* 2017;29:573–80.
35. Hirano Y, Arie T. PCR-based differentiation of *Fusarium oxysporum* ff. sp. lycopersici and radicis-lycopersici and races of *F. oxysporum* f. sp. lycopersici. *J Gen Plant Pathol.* 2006;72:273–83.
36. Jain D, Khurana JP. Role of pathogenesis-related (PR) proteins in plant defense mechanism. In: *Molecular aspects of plant-pathogen interaction.* Springer, Singapore; 2018. p. 265–81.
37. Johan MR, Suan MSM, Hawari NL, Ching HA. Annealing effects on the properties of copper oxide thin films prepared by chemical deposition. *Int J Electrochem Sci.* 2011;6:6094–104.
38. Juárez-Maldonado A, Tortella G, Rubilar O, Fincheira P, Benavides-Mendoza A. Biostimulation and toxicity: the magnitude of the impact of nanomaterials in microorganisms and plants. *J Adv Res.* 2021;31:113–26.
39. Kar M, Mishra D. Catalase, peroxidase, and polyphenoloxidase activities during rice leaf senescence. *Plant Physiol.* 1976;57:315–9.
40. Karlsson KR, Cowley S, Martinez FO, Shaw M, Minger SL, James W. Homogeneous monocytes and macrophages from human embryonic stem cells following coculture-free differentiation in M-CSF and IL-3. *Exp Hematol.* 2008;36:1167–75.
41. Karthik N, Edison TNJ, Sethuraman MG, Lee YR. Sonochemical fabrication of petal array-like copper/nickel oxide composite foam as a pseudocapacitive material for energy storage. *Appl Surf Sci.* 2017;396:1245–50.
42. Kataria N, Garg VK. Green synthesis of Fe₃O₄ nanoparticles loaded sawdust carbon for cadmium (II) removal from water: regeneration and mechanism. *Chemosphere.* 2018;208:818–28.
43. Kataria R, Ghosh S. NaOH pretreatment and enzymatic hydrolysis of Saccharum spontaneum for reducing sugars production. *Energy Sources Part A Recov Utiliz Environ Effects.* 2014;36:1028–35.
44. Keller AA, Lazareva A. Predicted releases of engineered nanomaterials: from global to regional to local. *Environ Sci Technol Lett.* 2014;1:65–70.
45. Khani R, Roostaee B, Bagherzade G, Moudi M. Green synthesis of copper nanoparticles by fruit extract of *Ziziphus spina-christi* (L.) Willd.: Application for adsorption of triphenylmethane dye and antibacterial assay. *J Mol Liq.* 2018;255:541–9.
46. Kohatsu MY, Pelegrino MT, Monteiro LR, Freire BM, Pereira RM, Fincheira P, Rubilar O, Tortella G, Batista BL, Araujo T, de Jesus. Comparison of foliar spray and soil irrigation of biogenic CuO nanoparticles (NPs) on elemental uptake and accumulation in lettuce. *Environ Sci Pollut Res.* 2021;28:16350–67.
47. Kumar P, Singhal VK, Kaur D. Impaired male meiosis due to irregular synapsis coupled with cytotoxicity in a new diploid cytotype of *Dianthus angulatus* (Caryophyllaceae) from Indian cold deserts. *Folia Geobot.* 2012;47:59–68.
48. Kumbhakar DV, Datta AK, Mandal A, Das D, Gupta S, Ghosh B, Halder S, Dey S. Effectivity of copper and cadmium sulphide nanoparticles in mitotic and meiotic cells of *Nigella sativa* L. (black cumin)—can nanoparticles act as mutagenic agents? *J Exp Nanosci.* 2016;11:823–39.
49. Laser KD, Lersten NR. Anatomy and cytology of microsporogenesis in cytoplasmic male sterile angiosperms. *Bot Rev.* 1972;38:425–54.
50. Li Z, Wang X, Liao T, Feng Q, Zhang D. A self-developed system for visual detection of vegetable seed vigor index. *Int J Agric Biol.* 2016;18:86–91.
51. Lichtenthaler HK. Chlorophyll fluorescence signatures of leaves during the autumnal chlorophyll breakdown. *J Plant Physiol.* 1987;131(1–2):101–110.
52. Liu WK, Yang Q-C, Lianfeng Du. Soilless cultivation for high-quality vegetables with biogas manure in China: feasibility and benefit analysis. *Renewable Agric Food Syst.* 2009;24:300–7.
53. Lopez-Lima D, Mtz-Enriquez AI, Carrión G, Basurto-Cereceda S, Pariona N. The bifunctional role of copper nanoparticles in tomato: Effective treatment for Fusarium wilt and plant growth promoter. *Sci Hortic.* 2021;277: 109810.
54. López-Vargas ER, Ortega-Ortiz H, Cadenas-Pliego G, de Alba K, Romenus MC, de la Fuente A, Benavides-Mendoza, and Antonio Juárez-Maldonado. Foliar application of copper nanoparticles increases the fruit quality and the content of bioactive compounds in tomatoes. *Appl Sci.* 2018;8:1020.
55. Lucini L, Baccolo G, Roupheal Y, Colla G, Bavaresco L, Trevisan M. Chitosan treatment elicited defence mechanisms, pentacyclic triterpenoids and stilbene accumulation in grape (*Vitis vinifera* L.) bunches. *Phytochemistry.* 2018;156:1–8.
56. Marmiroli M, Pagano L, Rossi R, De La Torre-Roche R, Lepore GO, Ruotolo R, Gariani G, Bonanni V, Pollastri S, Puri A. Copper oxide nanomaterial fate in plant tissue: nanoscale impacts on reproductive tissues. *Environ Sci Technol.* 2021;55:10769–83.
57. Mehriani K, Saeed RH, Rahmani F, Najafi S. Effect of chemical synthesis silver nanoparticles on germination indices and seedlings growth in seven varieties of *Lycopersicon esculentum* Mill (tomato) plants. *J Cluster Sci.* 2016;27:327–40.
58. Mosa MA, Youssef K. Topical delivery of host induced RNAi silencing by layered double hydroxide nanosheets: an efficient tool to decipher pathogenicity gene function of *Fusarium crown and root rot* in tomato. *Physiol Mol Plant Pathol.* 2021;115: 101684.
59. Mosa MA, El-Abeid SE, Khalifa MMA, Elsharouny TH, El-Baz SM, Ahmed AY. Smart pH responsive system based on hybrid mesoporous silica nanoparticles for delivery of fungicide to control *Fusarium crown and root rot* in tomato. *J Plant Pathol.* 2022;104:979–92.
60. Musheer N, Jamil A, Choudhary A. Solo and combined applications of fungicides and bio-agents to reduce severity of *Fusarium oxysporum* and induce antioxidant metabolites in *Ocimum tenuiflorum* L. *Journal of Plant Pathology.* 2023;105:237–51.
61. Nandakumar R, Babu S, Viswanathan R, Raguchander T, Samiyappan R. Induction of systemic resistance in rice against sheath blight disease by *Pseudomonas fluorescens*. *Soil Biol Biochem.* 2001;33:603–12.
62. Nasrollahzadeh M, Babaei F, Fakhri P, Jaleh B. Synthesis, characterization, structural, optical properties and catalytic activity of reduced graphene oxide/copper nanocomposites. *RSC Adv.* 2015;5:10782–9.
63. Nelson PE. *Fusarium species. An Illustrated Manual for Identification.* The Penn St. In.: University Press; 1983.
64. Noori A, Ngo A, Gutierrez P, Theberge S, White JC. Silver nanoparticle detection and accumulation in tomato (*Lycopersicon esculentum*). *J Nanopart Res.* 2020;22:1–16.
65. Peng F, Wang H, Hao Yu, Chen S. Preparation of aluminum foil-supported nano-sized ZnO thin films and its photocatalytic degradation to phenol under visible light irradiation. *Mater Res Bull.* 2006;41:2123–9.
66. Pradhan S, Patra P, Mitra S, Dey KK, Jain S, Sarkar S, Roy S, Palit P, Goswami A. Manganese nanoparticles: impact on non-nodulated plant as a potent enhancer in nitrogen metabolism and toxicity study both in vivo and in vitro. *J Agric Food Chem.* 2014;62:8777–85.
67. Ramamoorthy V, Raguchander T, Samiyappan R. Enhancing resistance of tomato and hot pepper to *Pythium* diseases by seed treatment with fluorescent pseudomonads. *Eur J Plant Pathol.* 2002;108:429–41.
68. Ramyadevi J, Jeyasubramanian K, Marikani A, Rajakumar G, Rahuman AA, Santhoshkumar T, Kirthi AV, Jayaseelan C, Marimuthu S. Copper nanoparticles synthesized by polyol process used to control hematophagous parasites. *Parasitol Res.* 2011;109:1403–15.
69. Rehana D, Mahendiran D, Senthil Kumar R, Kalilur A, Rahiman. Evaluation of antioxidant and anticancer activity of copper oxide nanoparticles synthesized using medicinally important plant extracts. *Biomed Pharmacother.* 2017;89:1067–77.
70. Rehman M, Saleem MH, Fahad S, Bashir S, Peng D, Deng G, Alamri S, Siddiqui MH, Khan SM, Shah RA. Effects of rice straw biochar and nitrogen fertilizer on ramie (*Boehmeria nivea* L.) morpho-physiological traits, copper uptake and post-harvest soil characteristics, grown in an aged-copper contaminated soil. *J Plant Nutr.* 2021;45:11–24.
71. Rodriguez MH, Bandte M, Gaskin T, Fischer G, Büttner C. Efficacy of electrolytically-derived disinfectant against dispersal of *Fusarium*

- oxysporum* and *Rhizoctonia solani* in hydroponic tomatoes. *Sci Hortic*. 2018;234:116–125.
72. Romberg MK, Davis RM. Host range and phylogeny of *Fusarium solani* f. sp. *eumartii* from potato and tomato in California. *Plant Dis*. 2007;91:585–92.
 73. Roncero M, Isabel G, Hera C, Ruiz-Rubio M, Garcia FI, Maceira MP, Madrid ZC, Calero F, Delgado-Jarana J, Roldán-Rodríguez R, Martínez-Rocha AL. *Fusarium* as a model for studying virulence in soilborne plant pathogens. *Physiol Mol Plant Pathol*. 2003;62:87–98.
 74. Sabrine H, Afif H, Mohamed B, Hamadi B, Maria H. Effects of cadmium and copper on pollen germination and fruit set in pea (*Pisum sativum* L.). *Sci Hortic*. 2010;125:551–5.
 75. Scruggs AC, Quesada-Ocampo LINAM. Etiology and epidemiological conditions promoting *Fusarium* root rot in sweetpotato. *Phytopathology*. 2016;106:909–19.
 76. Shenashen M, Derbalah A, Hamza A, Mohamed A, El Safty S. Recent trend in controlling root rot disease of tomato caused by *Fusarium solani* using aluminasilica nanoparticles. *Int J Adv Res Biol Sci*. 2017;4:105–19.
 77. Siddaiah CN, Satyanarayana NR, Mudili V, Gupta VK, Gurunathan S, Rangappa S, Huntrike SS, Srivastava RK. Elicitation of resistance and associated defense responses in *Trichoderma hamatum* induced protection against pearl millet downy mildew pathogen. *Sci Rep*. 2017;7:43991.
 78. Sonobe R, Yamashita H, Mihara H, Morita A, Ikka T. Estimation of leaf chlorophyll a, b and carotenoid contents and their ratios using hyperspectral reflectance. *Remote Sensing*. 2020;12:3265.
 79. Sperdouli I, Adamakis I-D, Dobrikova A, Apostolova E, Hanč A, Moustakas M. Excess zinc supply reduces cadmium uptake and mitigates cadmium toxicity effects on chloroplast structure, oxidative stress, and photosystem II photochemical efficiency in *Salvia sclarea* plants. *Toxics*. 2022;10:36.
 80. Sun L, Wang Y, Wang R, Wang R, Zhang P, Qiong Ju, Jin Xu. Physiological, transcriptomic, and metabolomic analyses reveal zinc oxide nanoparticles modulate plant growth in tomato. *Environ Sci Nano*. 2020;7:3587–604.
 81. Tanaka R, Tanaka A. Chlorophyll cycle regulates the construction and destruction of the light-harvesting complexes. *Biochimica Et Biophysica Acta (BBA) Bioenergetics*. 2011;1807:968–76.
 82. Tanase C, Boz I, Stingu A, Volf I, Popa VI. Physiological and biochemical responses induced by spruce bark aqueous extract and deuterium depleted water with synergistic action in sunflower (*Helianthus annuus* L.) plants. *Ind Crops Prod*. 2014;60:160–7.
 83. Tesso T, Ochanda N, Clafin L, Tuinstra M. An improved method for screening *Fusarium* stalk rot resistance in grain sorghum (*Sorghum bicolor* [L.] Moench.). *African J Plant Sci*. 2009;3:254–62.
 84. Tombuloglu H, Slimani Y, Tombuloglu G, Almessiere M, Baykal A. Uptake and translocation of magnetite (Fe₃O₄) nanoparticles and its impact on photosynthetic genes in barley (*Hordeum vulgare* L.). *Chemosphere*. 2019;226:110–22.
 85. Tombuloglu H, Slimani Y, AlShammari TM, Bargouti M, Ozdemir M, Tombuloglu G, Akhtar S, Sabit H, Hakeem KR, Almessiere M. Uptake, translocation, and physiological effects of hematite (α-Fe₂O₃) nanoparticles in barley (*Hordeum vulgare* L.). *Environ Pollut*. 2020;266:115391.
 86. Tripathi DK, Singh VP, Prasad SM, Chauhan DK, Dubey NK. Silicon nanoparticles (SiNp) alleviate chromium (VI) phytotoxicity in *Pisum sativum* (L.) seedlings. *Plant Physiol Biochem*. 2015;96:189–98.
 87. Velsankar K, Suganya S, Muthumari P, Mohandoss S, Sudhahar S. Ecofriendly green synthesis, characterization and biomedical applications of CuO nanoparticles synthesized using leaf extract of *Capsicum frutescens*. *J Environ Chem Eng*. 2021;9: 106299.
 88. Venkatachalam P, Priyanka N, Manikandan K, Ganeshbabu I, Indiraarulselvi P, Geetha N, Muralikrishna K, Bhattacharya RC, Tiwari M, Sharma NJPP. Enhanced plant growth promoting role of phycomolecules coated zinc oxide nanoparticles with P supplementation in cotton (*Gossypium hirsutum* L.). *Plant Physiol Biochem*. 2017;110:118–27.
 89. Vetter JL, Steinberg MP, Nelson AI. Enzyme assay, quantitative determination of peroxidase in sweet corn. *J Agric Food Chem*. 1958;6:39–41.
 90. Voitsekhovskaja OV, Tyutereva EV. Chlorophyll b in angiosperms: functions in photosynthesis, signaling and ontogenetic regulation. *J Plant Physiol*. 2015;189:51–64.
 91. Wierzbicka M, Panufnik D. The adaptation of *Silene vulgaris* to growth on a calamine waste heap (S. Poland). *Environ Pollut*. 1998;101:415–26.
 92. Xue Z, Liu P, Liu M. Cytological mechanism of 2 n pollen formation in Chinese jujube (*Ziziphus jujuba* Mill. 'Linglingzao'). *Euphytica*. 2011;182:231–8.
 93. Yallappa S, Manjanna J, Sindhe MA, Satyanarayan ND, Pramod SN, Nagaraja K. Microwave assisted rapid synthesis and biological evaluation of stable copper nanoparticles using T. arjuna bark extract. *Spectrochim Acta Part A Mol Biomol Spectrosc*. 2013;110:108–15.
 94. Yoshihara S, Yamamoto K, Nakajima Y, Takeda S, Kurahashi K, Tokumoto H. "Absorption of zinc ions dissolved from zinc oxide nanoparticles in the tobacco callus improves plant productivity", *Plant Cell. Tissue Organ Culture (PCTOC)*. 2019;138:377–85.
 95. Young M, Santra S. Copper (Cu)–Silica nanocomposite containing valence-engineered Cu: a new strategy for improving the antimicrobial efficacy of Cu biocides. *J Agric Food Chem*. 2014;62:6043–52.
 96. Zhang H, Ge L, Chen K, Zhao L, Zhang X. Enhanced biocontrol activity of *Rhodotorula mucilaginosa* cultured in media containing chitosan against postharvest diseases in strawberries: Possible mechanisms underlying the effect. *J Agric Food Chem*. 2014;62:4214–24.
 97. Zhao F-J, Ma Y, Zhu Y-G, Tang Z, McGrath SP. Soil contamination in China: current status and mitigation strategies. *Environ Sci Technol*. 2015;49:750–9.
 98. White TJ, Bruns T, Lee S, Taylor JW. Amplification and direct sequencing of fungal ribosomal RNA genes for phylogenetics. In: Innis MA, Gelfand DH, Sninsky JJ, White TJ, editors. *PCR Protocols: A Guide to Methods and Applications*. New York: Academic; 1990. p. 315–322.

Publisher's Note

Springer Nature remains neutral with regard to jurisdictional claims in published maps and institutional affiliations.